SEMMELWEIS EGYETEM

DOKTORI ISKOLA

Ph.D. értekezések

2897.

NAGY ÁKOS

Onkológia
című program

Program- és témavezető: Dr. Bödör Csaba, egyetemi tanár

Application of Circulating Tumor DNA Analysis for the Detection of *EZH2* Mutations in Follicular Lymphoma

PhD thesis

Ákos Nagy

Doctoral School of Pathological Sciences

Semmelweis University

Supervisor: Csaba Bödör, DSc

Official reviewers: Tibor Szarvas, DSc
Levente Kuthi, MD, PhD

Head of the Complex Examination Committee: Janina Kulka, MD, DSc

Members of the Complex Examination Committee: Dániel Erdélyi, MD, PhD

Budapest
2023

Table of contents

List of Abbreviations 5

I. Introduction 8

I.1. B-cells in the immune response 8

I.2. Classification of hematological neoplasms 10

I.3. Follicular lymphoma 10

I.3.1. Pathogenesis, genetic background 10

I.3.2. Diagnosis, prognosis 13

I.3.3. Patient Management 14

I.4. Liquid biopsy 16

I.5. Droplet digital PCR 18

II. Objectives 21

III. Methods 22

III.1. Sample recruitment and patient information 22

III.2. DNA isolation from LB samples 22

III.3. DNA isolation from TB samples 23

III.4. DNA isolation from PBMNC samples 23

III.5. Droplet digital PCR 23

III.6. Serial dilution 24

III.7. Data analysis and statistical methods 24

IV. Results 25

IV.1. *EZH2* mutation detection using a novel multiplex ddPCR assay 25

IV.2. *EZH2* mutation detection in TB and pre-treatment LB samples 27

IV.3. *EZH2* mutation detection in diagnostic and relapse samples 28

IV.4. Detection of intra- and inter-tumor heterogeneity 29

IV.5. Correlation of *EZH2* mutation status and VAF levels with histological, clinical and radiological parameters 33

IV.6. *EZH2* mutation detection in longitudinally collected follow-up LB samples ... 36

IV.7. Comparison of *EZH2* mutation analysis in LB and PBMNC specimens 40

V. Discussion 42

V.1. Development of the multiplex ddPCR assay 42

V.2. Analysis of *EZH2* mutations in classical TB and LB samples 43

V.3. Correlation between *EZH2* mutation status and allele burden and clinical variables 46

V.4. LB-based treatment monitoring in FL 47

V.5. *EZH2* mutation detection analysis comparing the cellular and acellular component of the blood 48

VI. Conclusions 49

VII. Summary 50

VIII. References 51

IX. Bibliography 64

X. Acknowledgements 66

List of Abbreviations

ABC-DLBCL	activated B-cell type diffuse large B-cell lymphoma
ABVD	doxorubicin, bleomycin, vinblastine, dacarbazine
AID	activation induced cytidine-deaminase
ASCT	autologous stem cell transplantation
BCR	B-cell receptor
BL	Burkitt lymphoma
BM	bone marrow
CD	cluster of differentiation
cfDNA	circulating cell-free DNA
cfRNA	circulating cell-free RNA
CNV	copy number variation
CPC	common progenitor cell
CTC	circulating tumor cell
ctDNA	circulating tumor DNA
ddPCR	droplet digital PCR
DLBCL	diffuse large B-cell lymphoma
DNA	deoxyribonucleic acid
dUTP	deoxyuridine triphosphate
EZH2	Enhancer of zeste homolog 2
EZH2i	EZH2 inhibitor
FFPE	formalin fixed paraffin embedded
FL	follicular lymphoma

FLIPI	FL international prognostic index
GCB-DLBCL	germinal center B-cell type diffuse large B-cell lymphoma
HL	Hodgkin lymphoma
Hyper-CVAD	Course A: cyclophosphamide, vincristine, doxorubicin, dexamethasone. Course B: methotrexate, cytarabine.
ICT	immunochemotherapy
IG	immunoglobulin
IGH	immunoglobulin heavy chain gene
LB	liquid biopsy
LDH	lactate dehydrogenase
LG	low-grade
LN	lymph node
LOD	limit of detection
MCL	mantle cell lymphoma
M-CLL	chronic lymphocytic leukemia with mutated BCR
mDNA	mitochondrial DNA
MT	mutant
MZL	marginal zone lymphoma
NGS	new generation sequencing
NHL	non-Hodgkin lymphoma
NPV	negative predictive value
ORR	objective response rate
PBMNC	peripheral blood mononuclear cells
PCM	plasma cell myeloma

PCR	polymerase chain reaction
PET/CT	18F-fluorodeoxyglucose positron emission tomography combined with computer tomography
R	rituximab
R/R	relapsed/refractory
R^2	rituximab-lenalidomide
RNA	ribonucleic acid
R-B	rituximab, bendamustine
R-CHOP	rituximab, cyclophosphamide, doxorubicin, vincristine, prednisolone
R-CVP	rituximab, cyclophosphamide, vincristine, prednisolone
R-DHAP	rituximab, dexamethasone, high-dose cytarabine, cisplatin
R-IGEV	rituximab, ifosfamide, gemcitabine, vinorelbine
SHM	somatic hypermutation
SUV max	maximum 18-fluorodeoxy glucose standardized uptake value
SV	structural variation
TB	tissue biopsy
tFL	transformed follicular lymphoma
TMTV	total metabolic tumor volume
U-CLL	chronic lymphocytic leukemia with unmutated BCR
VAF	variant allele frequency
V-D-J	variable, diversity, joining genes
WT	wild-type

I. Introduction

Owing to the unprecedented development of molecular laboratory techniques seen in the last fifty years, the genetic background of cancers had been mainly explored. These advancements opened a new era in the field of oncology, commonly referred to as personalized precision medicine. Several novel molecular biomarkers were described with a potential to aid diagnosis, prognostic risk stratification and treatment choice (predictive biomarkers), with some of these also acting as potential therapeutic targets (1).

Oncohematological diseases, mainly leukemias with circulating tumor cells in the blood, had always been the leading subjects of molecular investigations and advancements in medicine, owing to the ease of collecting genetic material from the tumor.

The discovery of tumor derived circulating cell-free deoxyribonucleic acid (cfDNA) in the blood plasma of oncology patients unlocked a novel field for medical and scientific research, namely liquid biopsy, hence similarly to leukemias, the tumor genetic material became relatively easily available (2). Unsurprisingly, solid tumors with great society burden (lung cancer, colorectal cancer, breast cancer etc.) were the leading subject of liquid biopsy-based studies in the past (3). Recently, oncohematological diseases, lacking circulating tumor cell components (lymphomas), have become one of the main targets of cfDNA-based research (4). My PhD work focused on potential applications of the liquid biopsy approach in one of the most common B-cell lymphoma subtype, follicular lymphoma.

I.1. B-cells in the immune response

The normal immune response is a complex process involving extensive changes in the genetic makeup of B- (and T-) cells, therefore carrying a risk for malignant transformation (5). It is considered that all B-cell derived malignancies can be attributed to a specific B-cell development stage in the physiological immune response (Figure 1). B-cells are produced by hematopoietic progenitor stem cells in the bone marrow (BM). Here, the random recombination of the of the immunoglobulin gene components (V-D-J recombination, V (variable), D (diversity), J (joining)) occurs, resulting in a naïve B-cell receptor (BCR) (6). These pre-B-cells then migrate to the lymphoid organs, where after

antigen exposure, they go through affinity maturation via somatic hypermutation (SHM) and class-switch recombination (6). Consequently, a highly antigen-specific B-cell clone is formed and selected, which will either differentiate to immunoglobulin (IG) producing plasma cell or into long-lasting memory B-cell.

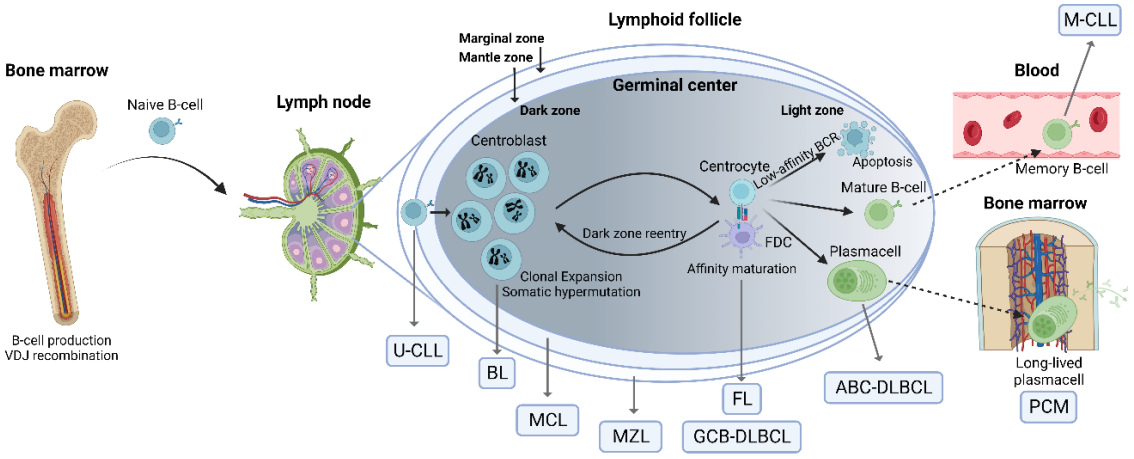

Figure 1. *B-cell development and cell of origin of B-cell malignancies. B-cells are produced in the bone marrow, where the recombination of the variable (V), diversity (D) and joining (J) genes occur forming the B-cell receptor (BCR). The naïve B-cells then migrate to the lymph nodes where they encounter with an antigen presented to them by follicular dendritic cells (FDC). After multiple cycles of dark zone entry and cell proliferation, the affinity of the BCR towards the antigen increases with via somatic hypermutation. Cells with low-affinity or self-reacting BCRs are eliminated during positive and negative selection. After the germinal center reaction B-cells with antigen specific BCRs participate in the physiological humoral immune response. After elimination of the pathogen these cells differentiate towards long-lived memory B-cells or plasma cells of the bone marrow. The genetic instability characterizing the reaction holds a significant oncogenic potential. Strikingly, each type of B-cell malignancy can be attributed to a physiological stage of B-cell development by histological and molecular features. ABC-DLBCL: activated B-cell type diffuse large B-cell lymphoma. BL: Burkitt lymphoma. FL: follicular lymphoma. GCB-DLBCL: germinal center B-cell type diffuse large B-cell lymphoma. MCL: mantle cell lymphoma. M-CLL: chronic lymphocytic leukemia with mutated BCR. MZL: marginal zone lymphoma. PCM: plasma cell myeloma. U-CLL: chronic lymphocytic leukemia with unmutated BCR. Created with BioRender.com.*

I.2. Classification of hematological neoplasms

The 5th edition of the Classification of Hematolymphoid Tumors released by the World Health Organization in 2022 separates the oncohematological malignancies into two big categories: myeloid and lymphoid malignancies. Within the latter, B-cell lymphoproliferative diseases are categorized into precursor, mature and plasma cell neoplasms (7). B-cell lymphomas, traditionally Hodgkin (HL) and non-Hodgkin lymphomas (NHL), are assigned to the mature B-cell neoplasms group (Figure 1).

I.3. Follicular lymphoma

Follicular lymphoma (FL) represents 5% of all hematological malignancies, it is the second most common NHL subtype after diffuse large B-cell lymphoma (DLBCL), accounting for 25% of all NHL cases (8). Moreover, it is most common indolent lymphoma in Western countries with an incidence rate of 2–4 per 100.000 capita-years (9). In Hungary, around 200 cases are diagnosed each year. FL is more common amongst the elderly, with a median age range of 60–65 years at the time of diagnosis. It is considerably more frequent in developed western societies, and it is more common among non-Hispanic white individuals compared to other ethnic groups in the United States (9).

FL has an indolent disease course, the overall survival can reach 15-20 years and the 5-year overall survival is 90% (10), however, the disease despite the modern immunochemotherapeutic approaches is still incurable. Moreover, FL is characterized by frequent relapses and high-grade histological transformation to the more aggressive DLBCL may occur in around 10% of the cases within five years after diagnosis (11). Given the incidence and the long overall survival, the prevalence of the disease in Hungary is around 2.000-2.500 cases.

I.3.1. Pathogenesis and genetic background

Based on its morphological and cellular features, FL is considered a prototypical tumor of germinal center origin. However, the pathognomic molecular event, namely the reciprocal translocation between chromosomes 14 and 18, occurs in pre-malignant naïve B-cells in the BM during the physiological V-D-J recombination (12). As a consequence of the translocation, the *BCL2* oncogene is placed under the transcriptional control of

immunoglobulin heavy chain (*IGH*) regulatory regions, leading to an ectopic overexpression of the antiapoptotic BCL2 protein. This molecular event decreases the apoptotic potential of these (pre)malignant cells, therefore B-cells with low affinity BCR evade apoptotic signals during positive selection (the process where B-cells with high-affinity BCRs are selected during affinity maturation) in the germinal center reaction. Even though the t(14;18) is a pathognomic event in the pathogenesis of FL and it occurs in 85% of all cases, it is not sufficient for malignant transformation, which requires additional genetic hits (13). Although, the presence of B-cells carrying the translocation in healthy individuals increases the risk of future malignant transformation to overt FL by around 23-fold (14), the majority of these individuals will never develop lymphoma, underlining that the translocation itself is not enough for malignant transformation (15).

Unlike normal B-cells, premalignant BCL2 positive cells enter the germinal center reaction multiple times during the disease evolution (due to their immortality caused by the aberrant expression of the antiapoptotic protein), where the somatic hypermutation process promotes a mutagenic environment and propagates clonal evolution towards malignant FL transformation (16). Early transformed FL clones are considered to carry early founding genetic mutations and thought to be the fundamental reservoir of further disease evolution and progression (8). These early malignant clones are usually referred to as common progenitor cells (CPC), and due to their central role in the disease subsequent progression, the isolation and selective eradication of these cells are the main targets of ongoing investigations. The above mentioned early founding genetic mutations in the CPCs are also present in clinically manifest FL tumor bulks with additional genetic hits.

Noteworthy, almost all FL cases carry at least one alteration in the epigenetic regulatory machinery (17), the most commonly affected genes are *KMT2D* (80%), *CREBBP* (70%), *EZH2* (25%) and *EP300* (20%) (18-20). These mutations will change the equilibrium between active and repressive histone marks of transcription, resulting in a shift from transcriptional activation towards aberrant repression of gene transcription. Other common FL specific mutation affects the *IGH* gene (80%), the *BCL2* gene (50%), transcription factors: *BCL6* (47%) and *MEF2B* (15%), tumor suppressors: *TNFAIP3* (26%) and *TNFRSF14* (25%) and tumor metabolism: *RRAGC* (17%) (19, 21).

The third most common mutation affecting the epigenetic system are the gain of function mutations of the *EZH2* gene (22, 23). The gene encodes a histone methyl-transferase enzyme, part of the polycomb repressive complex, which is responsible for transcriptional repression through methylating the histone 3 at 27th lysine residue (H3K27) (24, 25). The gain of function mutations of the gene results in an aberrant trimethylation of H3K27, further resulting in silencing of the target genes (Figure 2). There are seven different types of *EZH2* mutations in this disease affecting the catalytic set domain of the protein, located at exon16 (p.Y646N/F/C/H/S) and exon18 (p.A682G and p.A692V). These alterations are considered early clonal events therefore they are thought to be present in the CPC population as well, however cases with *EZH2* mutation restricted to disease progression or relapse were also described (19, 22, 26). The gain of function nature of these alterations proved to be an attractive pharmaceutical target, consequently tazemetostat, a first-in-its-class small molecular inhibitor of EZH2 has recently been approved in the US for the treatment of relapsed/refractory (R/R) FL with *EZH2* mutations (27), making EZH2 the first target in FL for precision oncology. The approval was based on an open-label, single-arm, multicenter, phase II trial, where patients with an *EZH2* mutation had an objective response rate (ORR) of 69%, meanwhile patients with wild-type *EZH2* had an ORR of only 35% (28). In line with these results, diagnostic tests able to detect these alterations reliably and sensitively represent a significant clinical need.

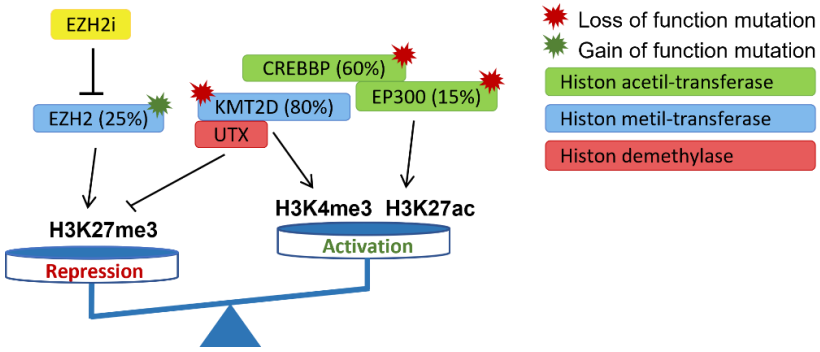

Figure 2. *Epigenetic dysregulation of transcription in follicular lymphoma. The disease is characterized by loss (KMT2D, CREBBP, EP300) and gain (EZH2) of function epimutations. These result in either aberrant transcriptional activation or repression of target genes through methylation or acetylation. EZH2 inhibitor (EZH2i) restores normal chromatin mark by suppressing the elevated EZH2 protein activity.*

The malignant transformation of premalignant t(14;18) positive cells to CPCs and eventually to FL cells requires several additional genetic hits acquired within years of slow progression during multiple re-entries to the germinal center reaction. This slow evolution results in a substantial clonal heterogeneity within an individual's tumor. This heterogeneity can be present at molecular, cellular and morphological level as well within one tumor bulk (intra-tumor heterogeneity) or between distinct tumor sites (inter-tumor heterogeneity) (29, 30). Moreover, the disease is also characterized by temporal heterogeneity, meaning that the genetic/morphological architecture of the tumor sites collected at diagnosis and relapse can substantially differ from each other.

I.3.2. Diagnosis and prognosis

FL usually presents with generalized painless lymph nodes, the most commonly affected regions are the cervical, axillar, inguinal and abdominal lymph nodes. Although the disease is often symptomless, it can also present with systemic symptoms including fatigue and B-symptoms (weight loss, fever, night sweats). The disease can infiltrate extranodal organs as well, most commonly the BM, resulting in anemia, recurrent infections and thrombocytopenia. Other affected extranodal organs can be the liver, the salivary glands, the skin, the duodenum and the spleen (8).

The cornerstone of the diagnosis remains the histopathological analysis, most commonly excisional or core biopsies are obtained from the affected lymph node regions. The tumor consists of enlarged homogenous neoplastic follicles, which can sometimes merge to form confluent nodules or diffuse areas of disease. By histopathological analysis, the tumor is CD20+ (cluster of differentiation 20), BCL2+, BCL6+, CD10+ (the activation induced cytidine-deaminase (AID) expression indicates the germinal center origin) and Ki67+ (being an indolent lymphoma, Ki67 proliferation marker is usually expressed in 20-30% of the cells). If the histological analysis is not conclusive, other ancillary test can help to establish the diagnosis, such as fluorescent in situ hybridization to detect the t(14;18), or examination of monoclonality by the analysis of the *IGH* gene (8). The pre-treatment diagnostic staging involves radiological imaging (most commonly 18F-fluorodeoxyglucose positron emission tomography combined with computer tomography (PET/CT), BM aspiration, routine blood tests and sometimes flow cytometry analysis to detect circulating tumor cells (CTC). The Ann-Arbor system is used for staging FL, where

limited stage (only one or more (stage I and II, respectively) regions are affected in one side of the diaphragm) or advanced stage (both sides are affected with or without BM involvement (stage IV and III, respectively)) can be distinguished (31).

Although FL responds well to modern treatments, the disease is incurable, and most patients will eventually experience relapse or disease progression. Therefore, accurate risk stratification prior to treatment represents an unmet clinical need. To date, several models have been proposed to predict treatment outcome, the most widely used one is the FL international prognostic index (FLIPI) incorporating five factors, namely age, stage, hemoglobin levels, lactate dehydrogenase (LDH) levels and number of involved nodal areas. Although this score was developed in the pre-rituximab era, it has maintained its validity (32). Taking advantage of the availability of whole genome sequencing results, a new prognostic model (m7-FLIPI) was created, incorporating clinical data and mutational status of seven genes (*EZH2*, *ARID1A*, *MEF2B*, *EP300*, *FOXO1*, *CREBBP* and *CARD11*) to predict treatment outcome of front-line immunochemotherapy regimens (R-CHOP (comprising rituximab, cyclophosphamide, doxorubicin, vincristine and prednisolone) or R-CVP (comprising rituximab, cyclophosphamide, vincristine and prednisolone)) (33). However, the usefulness of m7-FLIPI has not yet been proved in patients receiving bendamustine as chemotherapy backbone of rituximab (R-B).

I.3.3. Patient Management

About 20% of FL cases are diagnosed with limited stage (stage I/II) disease. Stage I and contiguous stage II (affected lymph nodes are in close proximity) disease can be treated with external beam radiation therapy alone (34). Asymptomatic patients, regardless of their stage, may not require treatment until symptomatic disease progression (watch and wait approach) (35). All other cases, including symptomatic advanced stage FL (80% of all cases), require systemic immunochemotherapy (ICT) regimens. The anti-CD20 rituximab monoclonal antibody revolutionized the treatment of B-cell NHLs, which is still the most widely used antibody in the management of FL. However, nowadays newer generations of anti-CD20 antibodies (e.g., obinutuzumab) with improved efficacy are also available (36). Even though, in selected cases, anti-CD20 therapy alone may be sufficient, it is usually combined with a chemotherapy backbone, the most common first-line regimens are R-B, R-CHOP and R-CVP. The choice between the regimens depends on

prognostic factors, physician's and patient's preference (37). After induction ICT, patients usually receive maintenance antibody treatment for two years every second months, since it improves progression free survival (38). An exciting chemo-free alternative is the rituximab-lenalidomide (R^2) combination which showed promising results in a phase III trial (39).

FL in the R/R setting can also be treated with the above-mentioned regimens. Cases with rapid progression and/or histological transformation are usually treated with autologous stem cell transplantation (ASCT). Several new treatment modalities are also available in the R/R setting, namely bispecific antibodies, chimera antigen receptor T-cell therapies, anti-CD47 antibody and small molecular inhibitors (PI3K inhibitors, HDAC inhibitors and the previously mentioned EZH2 inhibitor) (25, 37, 40).

Altogether, approximately 80% of the patients receive first-line ICT treatment. Progression within 24 months after initial systemic treatment occurs in 20% of these patients, which indicates poor prognosis and describes a patient group with highest need for novel treatment approaches (10). Around 40% of the patients will respond excellently to initial ICT and will achieve durable remission (>10 years). The last 40% of patients will relapse after two years and will experience the classical relapsing-remitting clinical course. This heterogeneous disease course requires effective patient follow-up and monitoring. Besides the routine blood test and physical examination performed at every patient-doctor encounter, the cornerstone of therapy monitoring nowadays is PET/CT imaging (41). During active ICT, one interim PET/CT is performed usually after the 4^{th} treatment cycle and one at the end of the treatment regimen. During maintenance therapy and treatment-free follow-ups, imaging is performed in 6-12 months intervals until 5 years from diagnosis.

However, PET/CT-based patient monitoring and evaluation is hampered by its limited specificity and sensitivity, leading to difficulties in interpreting cases with residual metabolic activity (42, 43). Therefore, novel tests able to detect minimal residual disease or emerging relapse-driving novel clones are needed. The most promising diagnostic alternative proved to be the liquid biopsy analysis so far.

I.4. Liquid biopsy

The term liquid biopsy refers to the molecular isolation, detection and analysis of cell-free nucleic acid-based biomolecules. Although, all kinds of body fluids can be utilized for liquid biopsy analysis, the blood plasma is by far the most commonly used source (44). From the blood plasma cfDNA, cell-free RNA (cfRNA) and mitochondrial DNA can selectively be detected and analyzed, however, cfDNA is the most common type of biomolecule used in this regard, owing to its relative stability (45) (Figure 3). Circulating cfDNA in the plasma was first discovered by Mendel and Metais in 1948 (46), although the potential clinical significance of these biomolecules were described only decades later. Typically, cfDNA molecules in the plasma have a short fragment length (~100-300 basepairs) and short half-life (~4-5 hours) owing to their renal and hepatic clearance and to plasma DNase enzymes (47). They are released to the blood by active secretion or passively from necrotic and apoptotic cells (the short fragment lengths are also the result of the cleavage of effector caspase enzymes). Healthy (cells of the BM, mucosa, parenchymal organs, and white blood cells) and tumor cells can either be the source of cfDNA. Therefore, the amount of cfDNA in the plasma is usually increased in patients with malignancies, this tumor-derived fraction of cfDNA is termed circulating tumor DNA (ctDNA), which can represent a wide proportion of all cfDNA molecules in the blood: it can vary between 0.01% to 90% (2). The molecular genetic alterations of the tumor are therefore mirrored in the ctDNA compartment as well; point mutations, copy number alterations, structural chromosome variations and methylation patterns can be investigated (Figure 3).

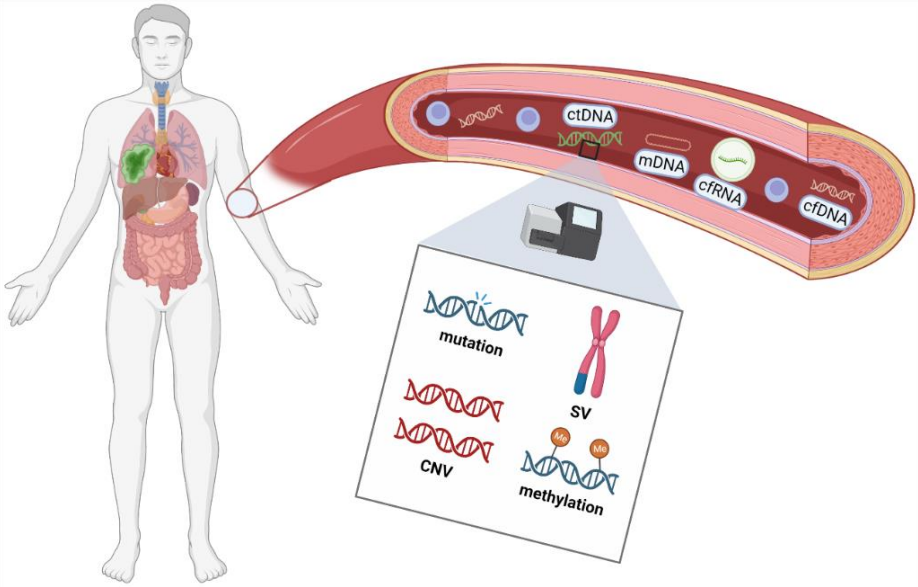

Figure 3. *Liquid biopsy. In the peripheral blood, several cell-free nucleic acid-based biomarkers can be found. Cell-free DNA (cfDNA) may originate from healthy or malignant tissues, with the latter usually referred to as circulating tumor DNA (ctDNA). Besides genomic DNA, mitochondrial DNA (mDNA) and exosome-bound cell-free RNA (cfRNA) molecules can also be found in the blood plasma. The molecular analysis of these biomolecules can reveal tumor specific genetic alterations, including mutations, copy number variations (CNV), structural variations (SV) and methylation patterns. Created with BioRender.com.*

Biomarker analysis for the diagnostic work-up of oncology patients can be performed on classical tissue biopsies (TB) or on liquid biopsies (LB). TB-based biomarker analysis has better analytical sensitivity, as usually large amount of DNA can be isolated from this sample type. The molecular and histological findings can also be aligned with each other when utilizing TBs. LB-based biomarker analysis, however, represents a painless, minimal invasive sample collection alternative, as a routine blood draw in a special collection tube is the only requirement. The minimal invasive nature allows for repeated sample collections, therefore longitudinal biomarker analysis during and after treatment is feasible with this method (3). Plasma cfDNA also represents the systematic disease because DNA fragments are shed to the bloodstream from all affected sites, therefore tumors with a considerable spatial heterogeneity, like FL, can be investigated (3) (Figure 3). LBs can also convey important molecular information from hard-to-biopsy tumors, e.g. tumors of the retroperitoneum or the central nervous system (48) (Figure 3).

Noteworthy, in older patient population, somatic molecular alterations owing to normal physiological aging of tissues (e.g. age-related clonal hematopoiesis in the BM) can easily be misinterpreted as false positive results in a LB specimen, hence caution and appropriately chosen analytical controls are required (49).

Nowadays, LB analysis is part of the diagnostic guidelines of non-small cell lung cancers and the screening guidelines of colorectal cancers (50, 51). In hematology, the most researched diseases in term of LB are DLBCL and HL. LBs have a potential in diagnostic, prognostic and predictive biomarker analysis and evaluation of general disease burden at the time of diagnosis, monitoring of treatment responses during therapy, and early detection of therapy resistance, minimal residual disease and emerging resistant clones after treatment (4).

The amount of cfDNA in the blood plasma is usually low (1-500 ng/ml), and as mentioned above, the tumor derived ctDNA fraction can be as low as 0.01% (45), especially in indolent diseases, like FL. Consequently, sensitive new generation molecular biology techniques are needed for analysis. The two, most commonly used methods are droplet digital PCR (ddPCR) and new generation sequencing (NGS).

I.5. Droplet digital PCR

The newest generation polymerase chain reaction (PCR), the ddPCR has an increased sensitivity compared to previous generation PCRs, which can reach 10^{-4} or 10^{-5}, meaning 0.01% or 0.001% variant allele frequencies (VAF) can be detected. As in real-time quantitative PCR set ups, ddPCR uses two fluorescent-labelled probes for allele specific detection. Unique to ddPCR, the reaction space is divided into ~10.000 independent reaction spaces by lipid particles. These distinct PCR reactions will individually be evaluated, therefore rare molecular events (e.g. mutations with low VAFs) can be detected with an increased statistical probability, hence the biological noise (wild-type DNA background) is decreased in the droplets carrying the alteration (52) (Figure 4). Beside the enhanced sensitivity, another advantage of this technique is the absolute quantification of the target DNA alleles, hence the original copy numbers can be calculated from the natural logarithm of the absolute number of empty droplets (droplets not carrying target DNA) (53). More than one target DNA molecule may be amplified in a single droplet,

therefore in some cases with enough input template DNA, a sensitivity below 10^{-4} can be achieved.

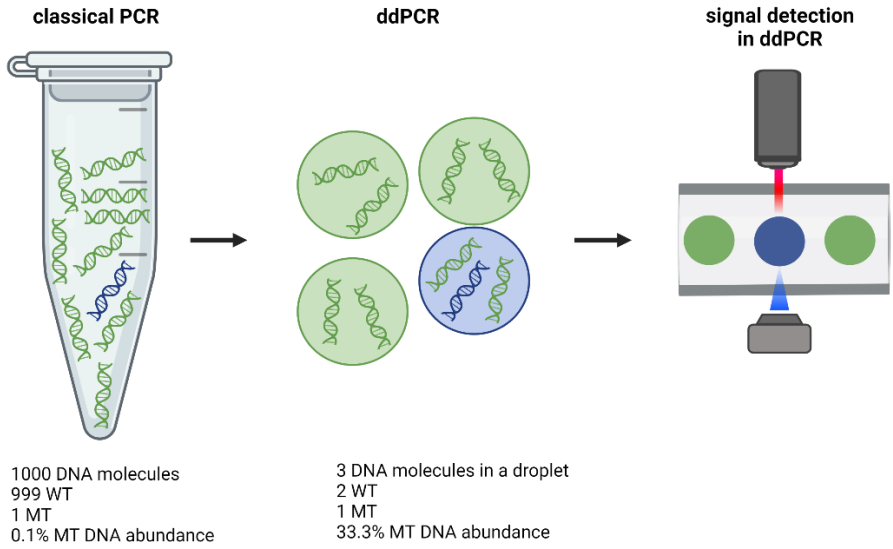

Figure 4. *Comparison of classical and digital droplet PCR (ddPCR) setups. In an ordinary PCR reaction, DNA fragments are amplified in the same reaction space, meanwhile in a ddPCR set up the reaction space is partitioned by lipid droplets into small, individual spaces where amplification will occur. The partitioning significantly increases sensitivity, hence in a droplet, the originally low abundancy of the mutant (MT) DNA molecule increases as the wild-type (WT) DNA background is decreased and the fluorescent signs of the droplets are eventually analyzed individually (in the figure, the relative abundancy is 300x in the ddPCR setup). Created with BioRender.com.*

Unlike NGS-based methods, where even whole genome or whole exom coverage can be reached, ddPCR is a low throughput technique, where usually only specific point mutations or the presence of distinct short sequences can be investigated. To overcome this limitation, multichannel ddPCR systems can be used, where each target can be labelled with distinct fluorophores (54). Several groups aimed to increase the detectable targets in a two-channel system by applying different concentrations from distinct target specific probes labelled with the same fluorophore (55, 56). By using this technique, targets labelled with a higher concentration of hydrolysis-probes will have a higher fluorescent intensity generating distinct fluorescent amplitude bands, consequently different targets labelled with the same fluorophore can be distinguished in a two-channel system as well. It is also noteworthy, that ddPCR is a relatively available cost-effective

solution for scenarios, where a known alteration or allele is aimed to be detected with a decent sensitivity.

II. Objectives

In my PhD work, we aimed to

1) Develop a cost-effective molecular biology test for the reliable and sensitive detection of *EZH2* mutations in follicular lymphoma with rapid turn-around time.
2) Determine the *EZH2* mutation frequency in a Hungarian FL patient cohort.
3) Investigate the spatial heterogeneity in FL: test the extent of intra- and inter-tumor heterogeneity in TBs and test the detectability of *EZH2* mutations from blood plasma samples. Compare the sensitivity and negative predictive value of LB and TB biopsy-based *EZH2* mutation analysis.
4) Investigate the temporal dynamics of *EZH2* mutations between diagnostic and relapse settings.
5) Scrutinize the correlation of *EZH2* mutation status and *EZH2* allele burden measured in the peripheral blood with clinical, pathological and radiological parameters.
6) Longitudinally monitor *EZH2* mutations in patients receiving immunochemotherapy.
7) Compare the detectability of *EZH2* mutations from the cellular (peripheral blood mononuclear cells (PBMNC)) and acellular (cfDNA) component of the blood.

III. Methods

III.1. Sample recruitment and patient information

Paired pre-treatment liquid biopsy (LB) and tumor biopsy (TB) samples were obtained from 117 FL patients treated in 10 Hungarian hematology centers. Seventy-eight patients were recruited at the time of diagnosis, thirty-eight at the time of relapse and one patient had paired TB and LB samples at both timepoints. Additionally, 84 LB samples were collected longitudinally at the first day of the treatment cycles from 24 patients (from the same cohort) being actively treated, with 2-7 sequential samples per patient. LB samples from 9 progressing/relapsed patients who lacked paired relapse TB samples were also included. Altogether, we analyzed 195 LB, 222 TB and 55 PBMNC samples collected from 126 FL patients. TB sample was available for 125 patients. *EZH2* mutation status from PBMNC samples (cellular component of the blood) was investigated if the corresponding LB sample collected at the same time proved to be *EZH2* mutant.

Relapse was defined as progression after at least one previous line of therapy or if the patient required treatment at least 12 months after watch and wait approach. The study was conducted in accordance with the Declaration of Helsinki, and the protocol was approved by the Ethics Committee of the Hungarian Medical Research Council (45371-2/2016/EKU and IV/5495-3/2021/EKU).

III.2. DNA isolation from LB samples

LB samples were collected using Cell-Free DNA Collection Tubes (Roche, Switzerland). Plasma fraction of 3-4 ml volume was isolated using a two-step centrifugation protocol (whole blood was centrifuged at 1.600 g for 20 min at 4 ^{o}C, subsequently the plasma fraction was centrifuged at 16.000 g for 10 minutes at 4 ^{o}C), then plasma samples were frozen at -70 ^{o}C until further processing. cfDNA was isolated using the QIAamp Circulating Nucleic Acid Kit (Qiagen, Germany) following the manufacturer's instructions. Isolated cell-free DNA samples were stored at -20 ^{o}C. Quantity and quality of cfDNA were assessed by Qubit 4 Fluorometer (Thermo Fisher Scientific, USA) and 4200 TapeStation System (Agilent Technologies, USA), respectively. Only those cfDNA samples were tested further, whose short fragment length (140-450 base pairs) ratio was above 80%, to avoid non-tumorous white blood cell DNA contamination.

III.3. DNA isolation from TB samples

Formalin fixed paraffin embedded (FFPE) TB samples were available from 125 patients. Altogether, 222 TB samples were collected (154 lymph nodes, 54 BM, 14 extranodal tissues). Tumor DNA from FFPE samples was isolated using the QIAamp DNA FFPE Tissue Kit (Qiagen, Germany). Isolated DNA samples were quantified by Qubit 4 Fluorometer (Thermo Fisher Scientific, USA) and stored at 4 ^{o}C.

III.4. DNA isolation from PBMNC samples

Mononuclear cell fraction of peripheral blood samples drawn into EDTA containing blood collection tubes was separated with Ficoll gradient centrifugation (400 g for 30 minutes). Cellular DNA was extracted using the MagCore Plus II Automated Nucleic Acid Extractor (RBC Bioscience Corporation, Taiwan). Isolated DNA samples were quantified by Qubit 4 Fluorometer (Thermo Fisher Scientific, USA) and stored at 4 ^{o}C.

III.5. Droplet digital PCR

EZH2 mutation status was determined with a QX200 ddPCR system (Bio-Rad Laboratories, USA). All PCR reactions were performed using ddPCR Supermix for probes (no deoxyuridine triphosphate (dUTP)) (Bio-Rad Laboratories, USA) for single PCR reactions and ddPCR Multiplex Supermix (Bio-Rad Laboratories, USA) for multiplex PCR reactions. We aimed to input 25 ng of template DNA into each reaction. Amplification was carried out in a C1000 Touch™ Thermal Cycler (Bio-Rad Laboratories, USA) with a standard ddPCR protocol. Reactions were accepted for subsequent analyses if at least 7.000 droplets were detected. Results were analyzed and translated to copy numbers/µl values and VAF using the QuantaSoft software (version 1.7; Bio-Rad Laboratories, USA).

We set up a unique multiplex PCR scenario capable of analyzing seven *EZH2* mutation hotspots in two distinct PCR reactions. In the first PCR reaction, we used four mutation-specific (*EZH2* p.Y646F/C/S and *EZH2* p.A682G) and two corresponding wild-type (WT) probes. In the second PCR reaction, three mutation-specific (*EZH2* p.Y646N/H and *EZH2* p.A692V) and two corresponding WT probes were used. A TB sample was considered mutant if the detected VAF was above 1%. The *EZH2* VAF values for all bone marrow samples were normalized for the tumor cell content (measured by flow

cytometry) using the following formula: VAF measured by ddPCR * (100/tumor content %). A VAF cut-off of 0.1% was applied for LB samples if the theoretical sensitivity was below this value, otherwise theoretical sensitivity was considered. The mean detected copy number was 333 copies/µl and 66 copies/µl, therefore the mean theoretical sensitivity of the ddPCR reactions were 0.03% and 0.15% for TB and LB samples, respectively. This was calculated from the reciprocal sum of mutant and wild type DNA fragments detected in 20 µl and multiplied by 100. All PBMNC samples were considered mutant if at least one droplet was positive for the tested mutation. If very few droplets (<2) supported the mutant *EZH2* status in a LB specimen the reaction was repeated.

III.6. Serial dilution

A PBMNC derived DNA mix pooled equimolarly from five healthy subjects was used to generate serial dilutions up to 100.000x from known *EZH2* mutant FFPE samples corresponding to the seven *EZH2* hotspots analyzed. To increase accuracy, additional dilution points were used (2.000x, 5.000x, 20.000x and 50.000x) beside the 10-fold dilution series points (10x, 100x, 1.000x, 10.000x, 100.000x). To determine the analytical sensitivity, PCR reactions near the sensitivity cut-off were run in triplicates for both single and multiplex ddPCR reactions. Sensitivity cut-off was identified if at least a single positive droplet was found in each triplicate.

III.7. Data analysis and statistical methods

Statistical analysis was performed using the Prism 8.0.1 software (GraphPad Software, Inc, USA). We investigated the statistical connection between the result *EZH2* mutation analysis and clinical parameters of the patients. Normal distribution of continuous variables was tested with the Shapiro-Wilk test. For the analysis of continuous variables, unpaired T-test, Mann-Whitney *U* test, one-way ANOVA or the Kruskal–Wallis one-way analysis of variance was used depending on the number of groups analyzed and on the distribution of variables. Categorical variables were studied with Chi-square test and Chi-square test for trend. The interdependence of two continuous variables was tested with linear regression. Paired variables and samples were tested with paired T-test, Wilcoxon signed-rank test and Friedman test depending on the number of groups analyzed and on the distribution of variables. All tests were two-sided, *p* value threshold for significance was set to 0.05% and 95% confidence interval was applied for all analyses.

IV. Results

IV.1. *EZH2* mutation detection using a novel multiplex ddPCR assay

First, we designed a novel multiplex droplet digital PCR approach for the simultaneous detection of distinct *EZH2* mutations. We performed a series of measurements with varying probe concentrations and combinations, resulting in an assay mix, which can stably and reproducibly detect the seven *EZH2* hotspot mutations in only two PCR reactions instead of performing seven distinct single PCR measurements. The resulting assay mix yields satisfactory separation in signal for each mutation. The two assay mixes generate up to 12 and 10 distinct fluorescent clusters upon applying to a pool of sample harboring each of the four and three somatic mutations plus WT DNA (Figure 5A-B).

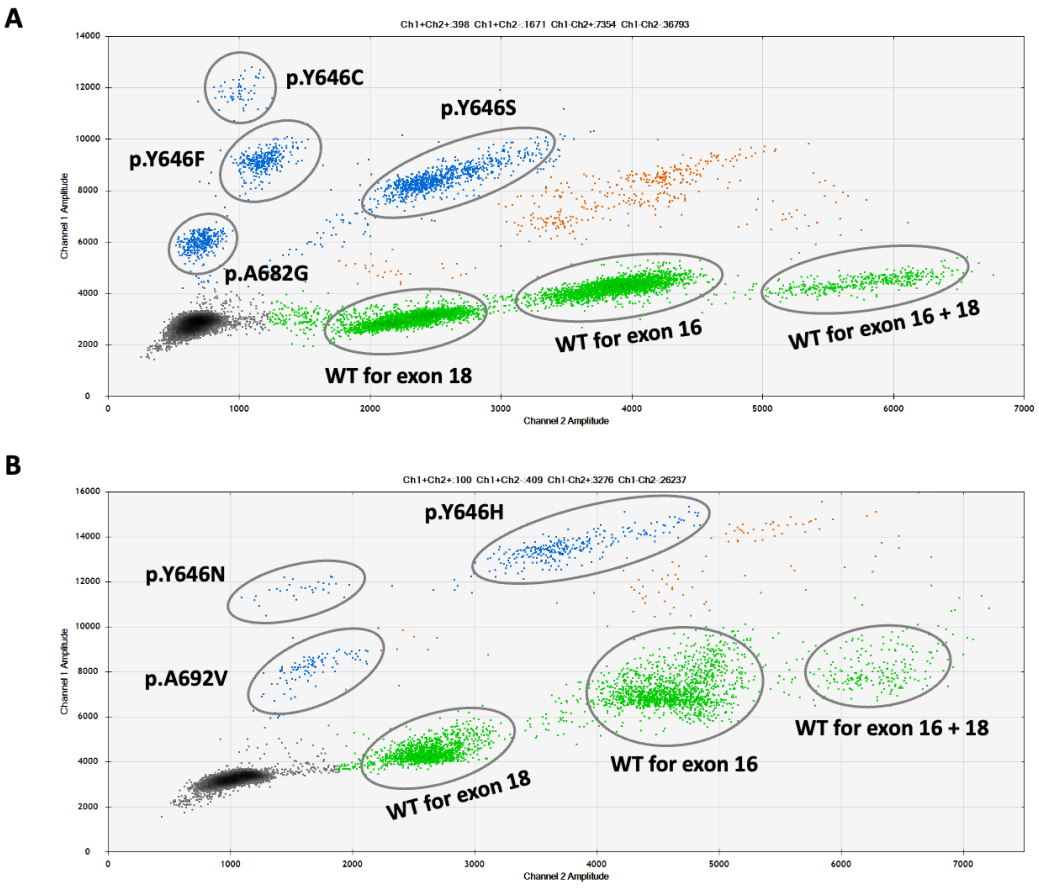

Figure 5. *Droplet digital PCR dotplots after applying the two multiplex assay mixes to a pool of samples harboring the corresponding four (**A**) and three (**B**) EZH2 mutations plus wild-type (WT) DNA. Fluorescent clusters harboring only one of the mutant DNA fragments are colored blue, droplets harboring WT DNA are colored green, clusters*

harboring both mutant and WT are colored orange, droplets without template DNA are grey. To determine the variant allele frequency of a mutation we selectively outlined the droplets containing the mutation with the „lasso" function of the QuantaSoft software, then similarly we outlined the corresponding WT droplets (WT for exon 16 and WT for exon 16 +18, if the mutation is p.Y646X and WT for exon 18 and WT for exon 16 + 18, if the mutation is p.A682G or p.A692V).

Competition between probes used in the same multiplex PCR amplification reaction may affect sensitivity. To detect and analyze the rate of this phenomenon, we made serial dilutions of FFPE samples known to harbor one of the seven *EZH2* mutation. We compared the limit of detection (LOD) of single vs multiplex PCR amplification for all alteration. With regards to all analyzed hotspots, no statistical difference was found between the single and multiplex PCR approach (paired T-test, p=0.75). Upon analyzing all hotspots individually, we have not found a difference in the LOD for mutation specific assays of p.Y646N/F/C/S and p.A682G, however, we detected decreased LOD for p.Y646H and p.A692V assays in the multiplex PCR setup, although neither exceeded one log difference and the analytical sensitivity remained below 0.1% for these targets as well. Upon comparing LB-based to TB-based *EZH2* analysis, we found that the LB-based approach slightly outperforms the TB-based one in terms of sensitivity and negative predictive value (NPV) (Figure 6A-B).

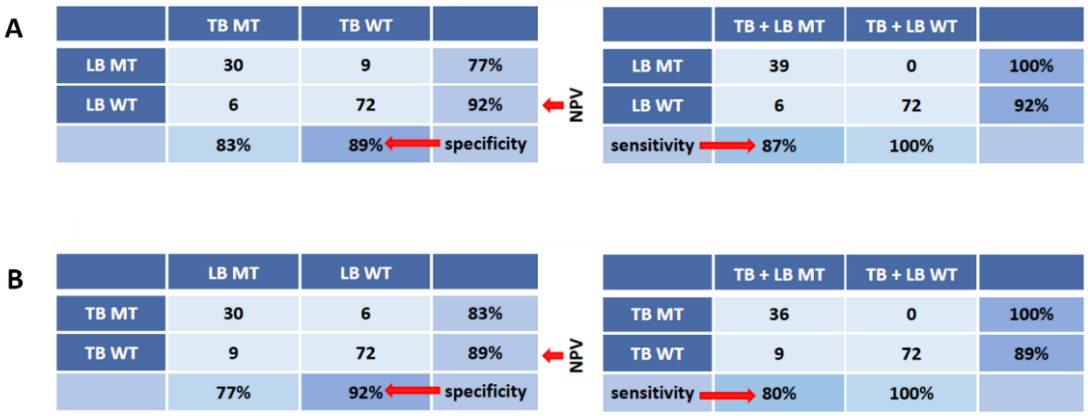

Figure 6A-B. *Comparison between statistical sensitivity, specificity and negative predictive value (NPV) of liquid biopsy (LB) and tissue biopsy (TB) based EZH2 mutation detection analysis of the 117 patients with paired TB and LB samples. We determined the specificity and the NPV of the TB- and the LB-based EZH2 mutation detection compared*

to the LB or to the TB-based approach, respectively. We did not consider those samples false positive where the EZH2 mutation was only found in the LB sample, therefore statistical sensitivity was calculated from the sum of mutant samples in TB and LB. MT: mutant. WT: wild-type.

We also scrutinized if the multiplex approach affects the detected VAF compared to the single PCR approach. First, three experienced members of our group compared the measured VAF for all seven hotspot mutations after multiplex PCR in 57 TB and LB samples, among 3 carrying two distinct *EZH2* mutations, and no significant difference was found between each observer (Mann-Whitney *U* test, p=0.72). Second, we compared the average VAF of the multiplex approach determined by the three independent observers to the VAF of the same samples determined by single PCR approach and again, no statistical difference was found (Friedman test, p=0.31).

IV.2. *EZH2* mutation detection in TB and pre-treatment LB samples

EZH2 mutations were detected in 42.1% (53/126) of the patients when considering all available sample types (diagnostic TB, relapse TB or pre-treatment LB specimen (Figure 7A). Analyzing the paired TB-LB samples (n=117), the *EZH2* mutation frequency was 38.4% (45/117) and it did not differ significantly between the TB and the LB samples (30.7% vs 33.3%, respectively, Chi-square test, p=0.68). However, in six patients (5.1%) the *EZH2* mutation was detected exclusively in the TB samples, while in nine (7.7%) patients, the *EZH2* mutation was only detected in the corresponding LB sample (Figure 7B). In this cohort, 53 different mutations were found in 45 patients. Among these 53 mutations, 30 mutations were present in both compartments, with 9 and 14 were only present in the TB or in the LB, respectively.

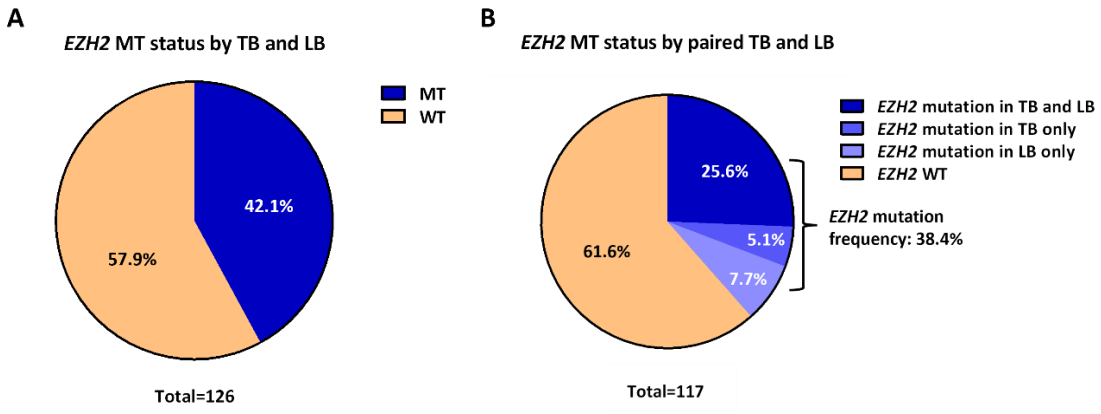

Figure 7. A: *EZH2 mutation (MT) status in all investigated samples.* ***B:*** *EZH2 MT status in patients with paired tissue (TB) and pre-treatment liquid biopsy (LB) samples. Patients harboring mutation exclusively in one compartment (TB or LB only) are displayed individually. WT: wild-type.*

Spectrum of *EZH2* mutations in liquid and tissue biopsy samples is summarized in Figure 8A. We did not find any difference between the spectrum of *EZH2* mutation types in TB and LB samples. Interestingly, we found a relative increase in the proportion of p.Y646N and decrease in the proportion of p.Y646F and p.Y646H mutations at the time of relapse (Figure 8B). Median *EZH2* mutation VAF was 21.5% (range 1.0 – 54.6%) and 2.3% (range 0.1 – 74%) in TB samples and in pre-treatment LB samples, respectively.

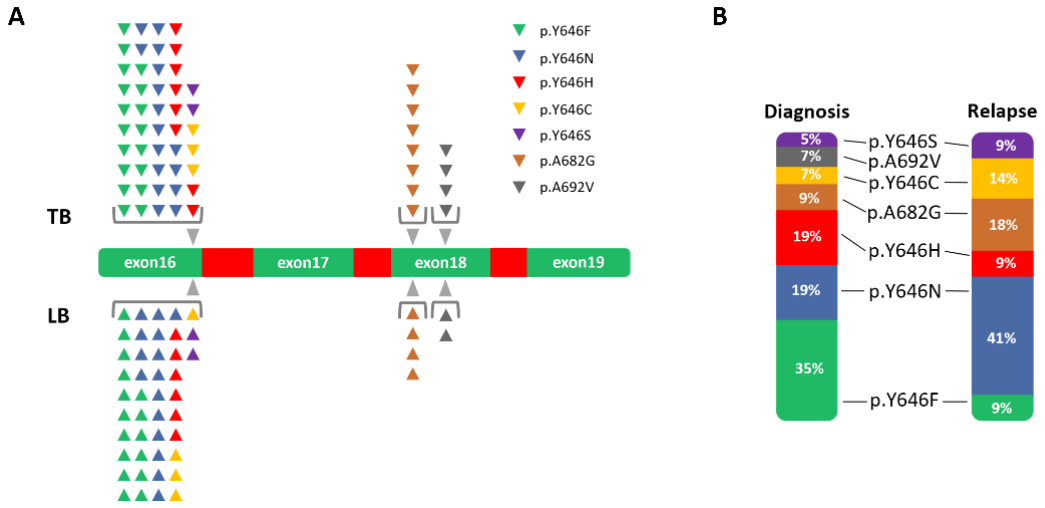

Figure 8. A: *Distribution of SET domain EZH2 mutation types in EZH2 mutant patients with paired tissue (TB) and liquid biopsy (TB).* ***B:*** *Distribution of SET domain EZH2 mutation types in samples collected at the time of diagnosis and at relapse.*

IV.3. *EZH2* mutation detection in diagnostic and relapse samples

With a median follow-up time of 29 months (range: 6-229), 50 patients (39.7%) relapsed after treatment or progressed after at least 12 months of watch and wait approach. From these 50 patients, 39 had an *EZH2* mutation analysis both at the time of diagnosis and relapse/progression from at least one sample of any kind (pre-treatment LB or TB). Although there was no significant difference in the *EZH2* mutation frequency between diagnosis and relapse (25.7% vs 41%, respectively, Chi-square test, p=0.15) we observed a switch in the *EZH2* mutation status during the disease course in 14 patients out of the

39 (35.9%) who had paired diagnostic and relapse samples available (4 *EZH2* wild-type relapse after *EZH2* mutant FL at diagnosis and 10 *EZH2* mutant relapse following *EZH2* wild-type diagnosis). Concordant mutant or wild-type *EZH2* mutation status comparing the diagnostic and relapse samples was detected in 6 and 19 patients, respectively. In four patients with paired diagnostic and relapse nodal TB, the measured *EZH2* VAF significantly increased at the time of relapse (paired T-test, p=0.02, Figure 9C). Altogether, 51.3% of relapsed patients in this cohort with paired diagnostic and relapse samples harbored an *EZH2* mutation at one point during the disease course (Figure 9A-B).

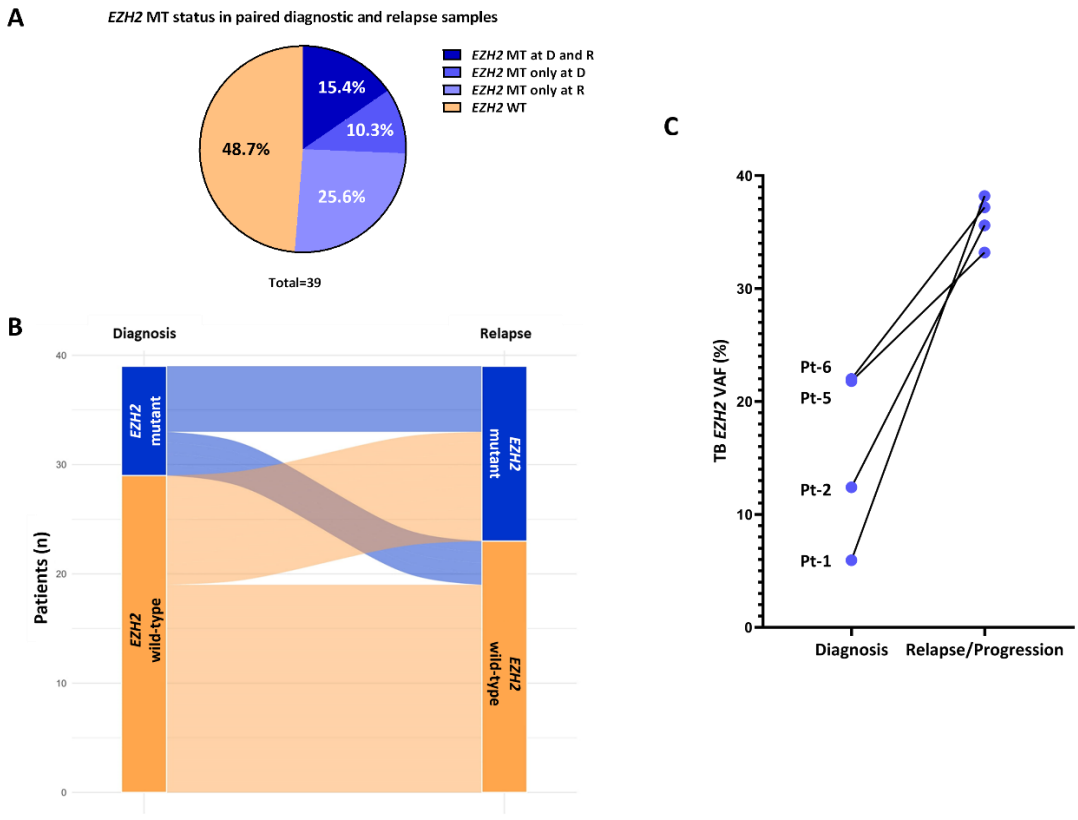

Figure 9. A*: Combined EZH2 mutation frequency in patients with paired diagnostic and relapse samples.* ***B****: EZH2 mutation status switch phenomenon in patients with paired diagnostic and relapse sample.* ***C:*** *Comparison of EZH2 VAFs between diagnosis and relapse in four patients with paired mutant TBs.*

IV.4. Detection of intra- and inter-tumor heterogeneity

Multiple TB samples collected at the same time from distinct sites were available from 54 patients. Spatial heterogeneity was documented in 8 patients (15%), in cases where

different *EZH2* mutation types were detected in distinct sites, or in patients with at least one mutant and one wild-type tumor site (Figure 10). Intra-tumoral heterogeneity was identified in 5.4% (3/56) of all nodal mutant TB samples, where at least two *EZH2* mutations were detected from the same sample. Multiple *EZH2* mutations were found in 14% of pre-treatment LB samples (6/43), again reflecting inter-tumoral spatial heterogeneity (Figure 11).

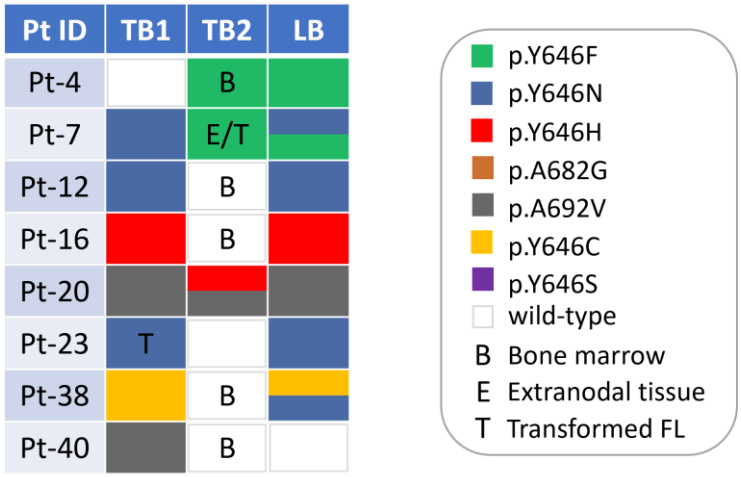

Figure 10. *Illustration of spatial heterogeneity captured in paired multiple tissue (TB) and liquid biopsy (LB) specimens of 8 patients. Multiple EZH2 mutations found in the same specimen are also indicated.*

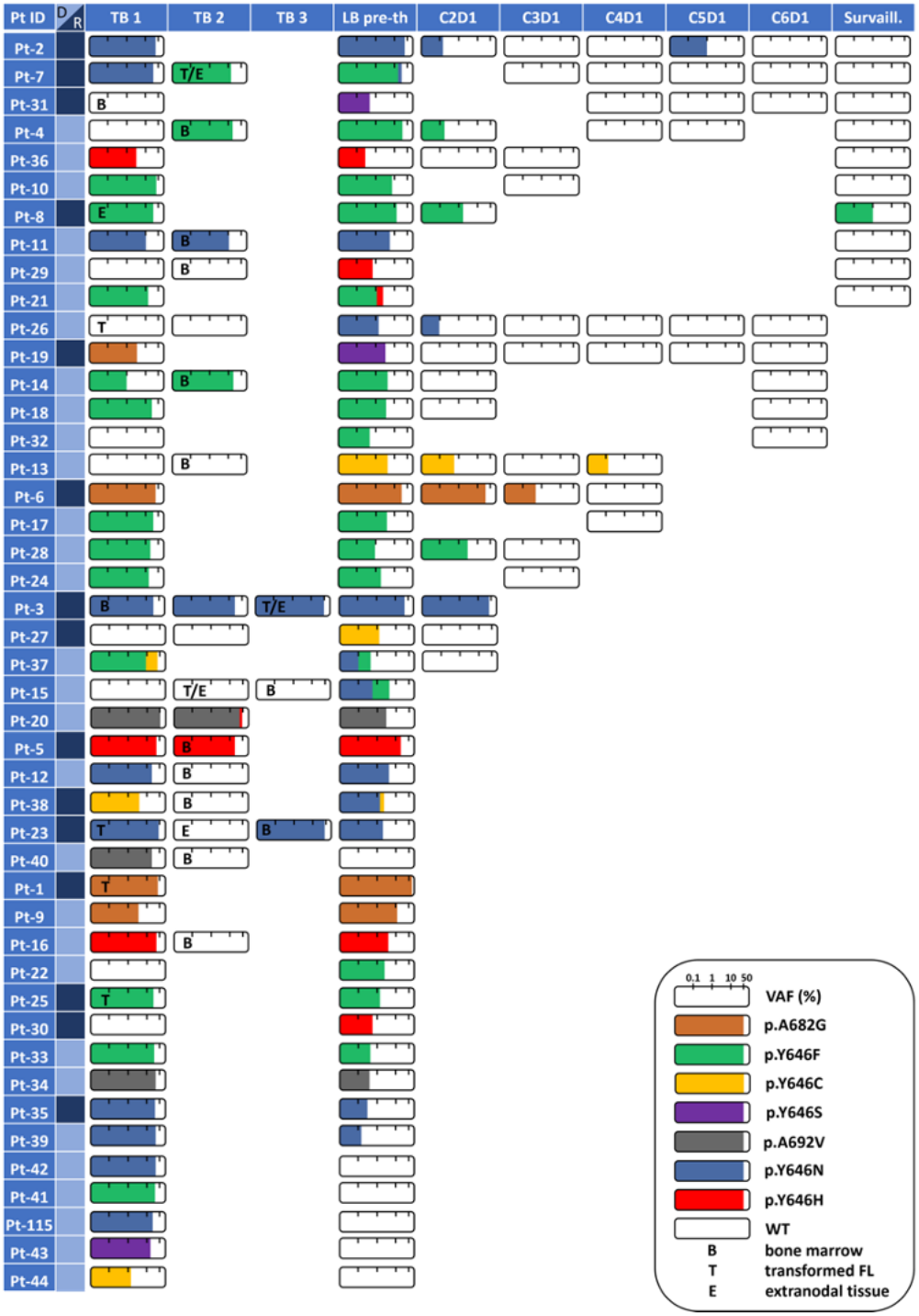

Figure 11. *EZH2 mutation pattern in 45 mutant follicular lymphoma patients with paired tissue (TB) and liquid biopsy samples (LB). Saturation of the bars represent variant allele frequencies (VAF) in a log2 scale. EZH2 VAFs (range: 0.1-74.0%) were multiplied by 100 (to avoid zero and minus values), then transformed to a log2 scale. Subsequently, each value was converted to percentage for illustration, where 100% VAF would occur as a fully saturated bar. C2D1: cycle 2 day 1. C3D1: cycle 3 day 1. C4D1: cycle 4 day 1.*

C5D1: cycle 5 day 1. C6D1: cycle 6 day 1. D: diagnosis. Pre-th: pre-treatment. R: relapse. Surveill: surveillance sample (LB sample collected at remission). WT: wild-type.

In Pt-7, two distinct *EZH2* mutations (p.Y646F and p.Y646N) were detected in the peripheral blood with different VAFs (20.4% and 0.4%, respectively). The analysis of the TBs proved that the p.Y646N mutation originated from a low-grade FL in the inguinal lymph nodes, meanwhile the p.Y646F mutation was found in an extranodal transformed FL from the duodenum wall (Figure 12A). Similarly, Pt-38 displayed two different mutations (p.Y646C and p.Y646N) in the LB specimen, however here, only the *EZH2* p.Y646C mutation was detected in the TB (in a cervical lymph node). This patient had a large retroperitoneal and mediastinal mass on PET/CT, which raises the possibility that the *EZH2* p.Y646N mutant clone was restricted to this, unbiopsied site (Figure 12B).

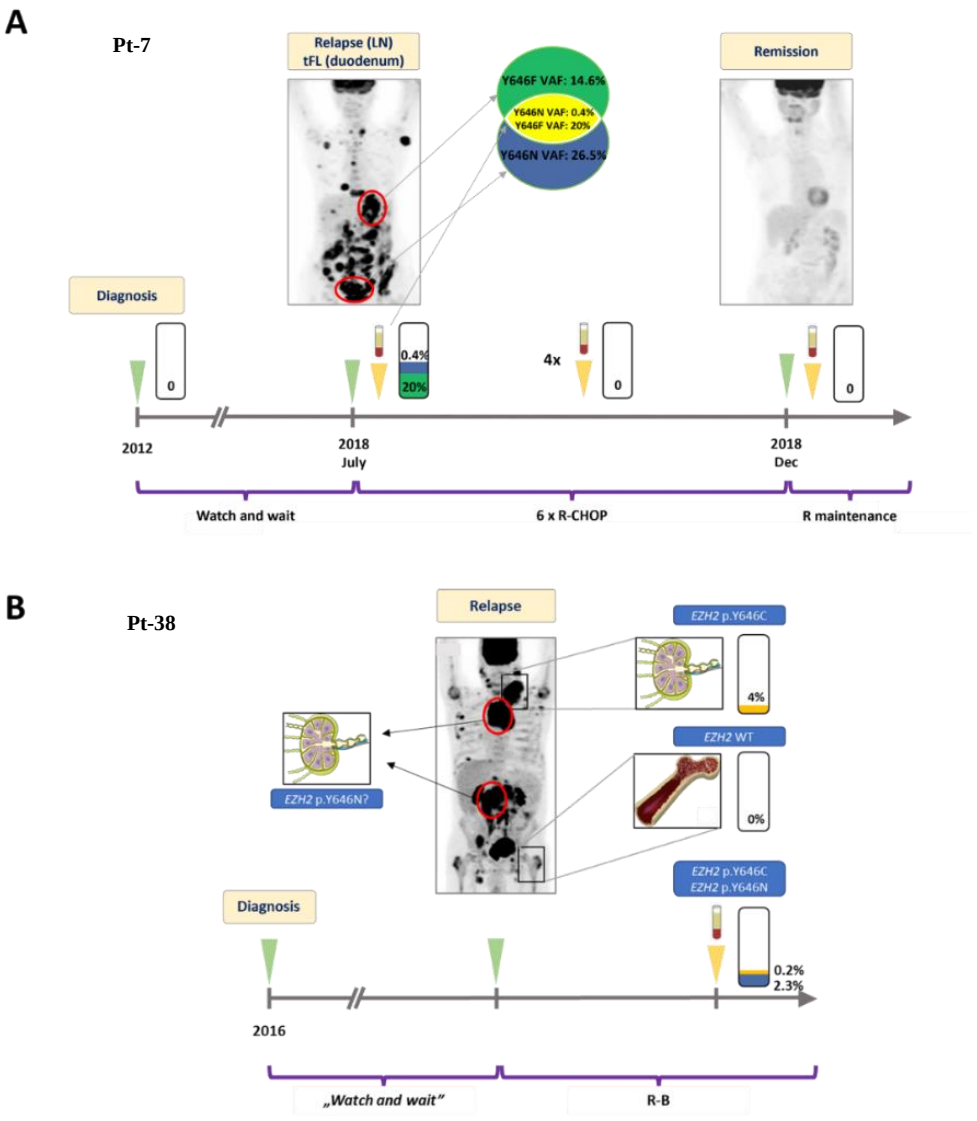

Figure 12. A*: Illustration of spatial heterogeneity and longitudinal treatment monitoring with liquid biopsy in the case of Pt-7. At the time of disease progression, a low- and a high-grade disease site was described by histological and molecular analysis. Both disease sites harbored a distinct EZH2 mutation, with both mutations recovered in the pre-treatment liquid biopsy specimen. These mutations rapidly eliminated from the blood after initiation of a successful treatment.* ***B****: Illustration of spatial heterogeneity in the case of Pt-38. At the time of relapse, a subclonal EZH2 mutation was found in the TB of the patient, with an additional EZH2 mutation present in the paired liquid biopsy sample. Extensive involvement of the mediastinal and retroperitoneal region was found on imaging, which unbiopsied regions may have been the source of the additional p.Y646N mutation found in the peripheral blood. Numbers in the rectangles represent the variant allele frequencies (VAF) of the mutations. LN: lymph node. tFL: transformed follicular lymphoma. R-B: rituximab, bendamustine. R-CHOP: rituximab, cyclophosphamide, doxorubicin, vincristine, prednisone. R: rituximab.*

IV.5. Correlation of *EZH2* mutation status and VAF levels with histological, clinical and radiological parameters

Altogether, we analyzed 222 TB samples collected from 125 patients at the time of diagnosis or at relapse. Upon comparing the *EZH2* mutation status and the *EZH2* VAF levels with histological grade, we found that higher histological grade is significantly associated with mutant TB *EZH2* status (Chi-square test, p=0.04) (Figure 13A) and higher TB *EZH2* VAF level (unpaired T-test, p=0.006) (Figure 13D) but we found only a trend with LB *EZH2* VAF level (Mann-Whitney U test, p=0.24) (Figure 13E). Similarly, we could only reveal a trend with linear regression analysis upon comparing corresponding TB and LB *EZH2* VAFs (Figure 13J). However, the highest *EZH2* VAF in a LB sample (74%) was measured in a case, who experienced early high-grade transformation following ICT (Pt-1), and eventually succumbed to the disease one week after sample collection (Figure 14).

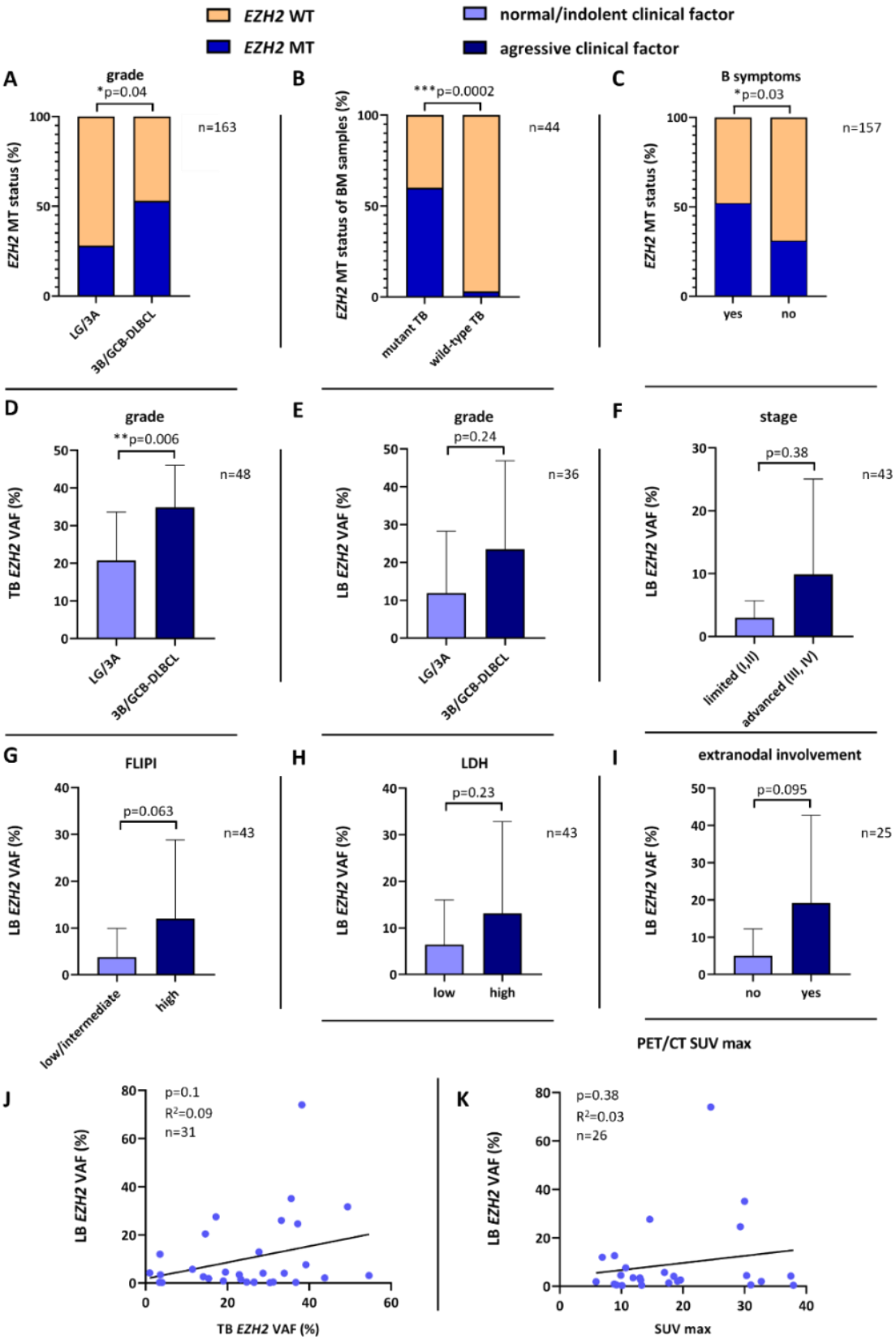
EZH2 WT
EZH2 MT
normal/indolent clinical factor
agressive clinical factor
A
grade
*p=0.04
n=163
EZH2 MT status (%)
LG/3A
3B/GCB-DLBCL
B
***p=0.0002
n=44
EZH2 MT status of BM samples (%)
mutant TB
wild-type TB
C
B symptoms
*p=0.03
n=157
EZH2 MT status (%)
yes
no
D
grade
**p=0.006
n=48
TB EZH2 VAF (%)
LG/3A
3B/GCB-DLBCL
E
grade
p=0.24
n=36
LB EZH2 VAF (%)
LG/3A
3B/GCB-DLBCL
F
stage
p=0.38
n=43
LB EZH2 VAF (%)
limited (I,II)
advanced (III, IV)
G
FLIPI
p=0.063
n=43
LB EZH2 VAF (%)
low/intermediate
high
H
LDH
p=0.23
n=43
LB EZH2 VAF (%)
low
high
I
extranodal involvement
p=0.095
n=25
LB EZH2 VAF (%)
no
yes
J
p=0.1
R²=0.09
n=31
LB EZH2 VAF (%)
TB EZH2 VAF (%)
K
p=0.38
R²=0.03
n=26
LB EZH2 VAF (%)
PET/CT SUV max
SUV max

Figure 13. A-K: *Correlation between EZH2 mutation status, EZH2 variant allele frequencies (VAF) and histological and clinical variables. P values marked with an asterix indicates statistically significant differences. Parenchymal organ or skin involvements were considered as extranodal involvement, bone marrow infiltration was evaluated separately. BM: bone marrow. FLIPI: follicular lymphoma international prognostic index. GCB-DLBCL: germinal center B-cell like diffuse large B-cell lymphoma. LB: liquid biopsy. LDH: lactate dehydrogenase. LG: low grade. MT: mutant/mutation. PET/CT: 18F-fluorodeoxyglucose positron emission tomography combined with computer tomography. SUV max: maximum 18-fluorodeoxy glucose standardized uptake value. TB: tissue biopsy. VAF: variant allele frequency. WT: wild-type.*

Interestingly, we found that wild-type *EZH2* status may be associated with increased risk of BM infiltration, although this did not reach statistical significance (Chi-square test, p=0.08). However, histologically confirmed BM infiltrates (with a median 17.5% infiltration by tumor cells) were more frequently *EZH2* wild-type, regardless of the mutation status of the paired TB: only six out of the ten patients with paired mutant TB displayed an *EZH2* mutation in the BM as well. On the contrary, only one patient harbored an *EZH2* mutation in the BM among the 34 patients with paired wild-type. Altogether, 16% (7/44) of infiltrated BM samples harbored the mutation, meanwhile 84% (37/44) proved to be *EZH2* wild-type.

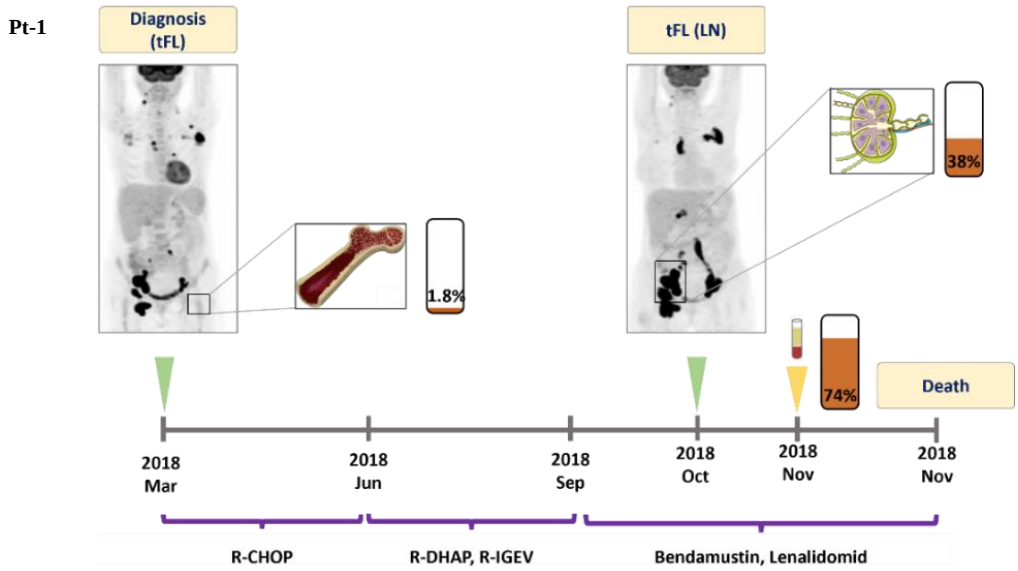

Figure 14. *Detailed illustration of Patient-1. Liquid biopsy obtained one week prior to the death of the patient revealed high variant allele frequency (VAF) of EZH2 p.A682G mutation. Numbers in the rectangles represent the VAF of the mutation. LN: lymph node, BM: bone marrow, tFL: transformed follicular lymphoma. R-CHOP: rituximab, cyclophosphamide, doxorubicin, vincristine, prednisone. R-DHAP: rituximab, dexamethasone, high-dose cytarabine, cisplatin. R-IGEV: rituximab, ifosfamide, gemcitabine, vinorelbine.*

The presence of B-symptoms was also significantly (Chi-square test, p=0.03) associated with mutant *EZH2* status (Figure 13C). There was no difference between median *EZH2* VAF at the time of diagnosis and progression/relapse (2.5% vs 2.2%, Mann-Whitney U test, p=0.13). The *EZH2* mutation status and the LB *EZH2* VAF level did not correlate with any of the other parameter analyzed, however, we found a trend between LB *EZH2* VAFs and clinical stage, FLIPI, LDH levels, presence of extranodal involvement and PET/CT SUV max (maximum 18-fluorodeoxy glucose standardized uptake value) value, where the group(s) with higher mean VAFs was associated with more aggressive clinical factors (Figure 13F-K).

IV.6. *EZH2* mutation detection in longitudinally collected follow-up LB samples

Follow-up LB samples collected on the first day of each treatment cycle were available from 24 patients. Among these, 19 patients were treated with first line immunochemotherapy (13 received R-B, 6 R-CHOP) or chemotherapy (Pt-36 was diagnosed with composite HL and FL, and was treated with ABVD (doxorubicin, bleomycin, vinblastine and dacarbazine)). All patients treated with first line regimen responded to treatment. At the time of sample collections 4 patient received therapy due to relapsed FL; 2 patients received R-CHOP, 1 R-DHAP (rituximab, dexamethasone, high-dose cytarabine, cisplatin) and 1 R^2 and altogether 3 out of 4 patients responded to the applied therapy.

Mean *EZH2* VAF was 9.2% and 5.12% before treatment and at the time of C2D1, respectively (Figure 15A). The difference between C1D1 and C2D1 VAF was not significant (Wilcoxon signed-rank test, p=0.06), although we observed a strong correlation upon analyzing only those patients that responded to ICT (9.2% vs 0.2%) (Wilcoxon signed-rank test, p=0.005) (Figure 15B). *EZH2* VAF significantly decreased

at the beginning of all subsequent cycles compared to C1D1 (Figure 15B). Patients responding to therapy were characterized by a prompt decrease in the *EZH2* VAF level after the initiation of treatment, meanwhile this did not happen in Pt-3, Pt-6, and Pt-28 who initially did not show clinical response (Figure 15C).

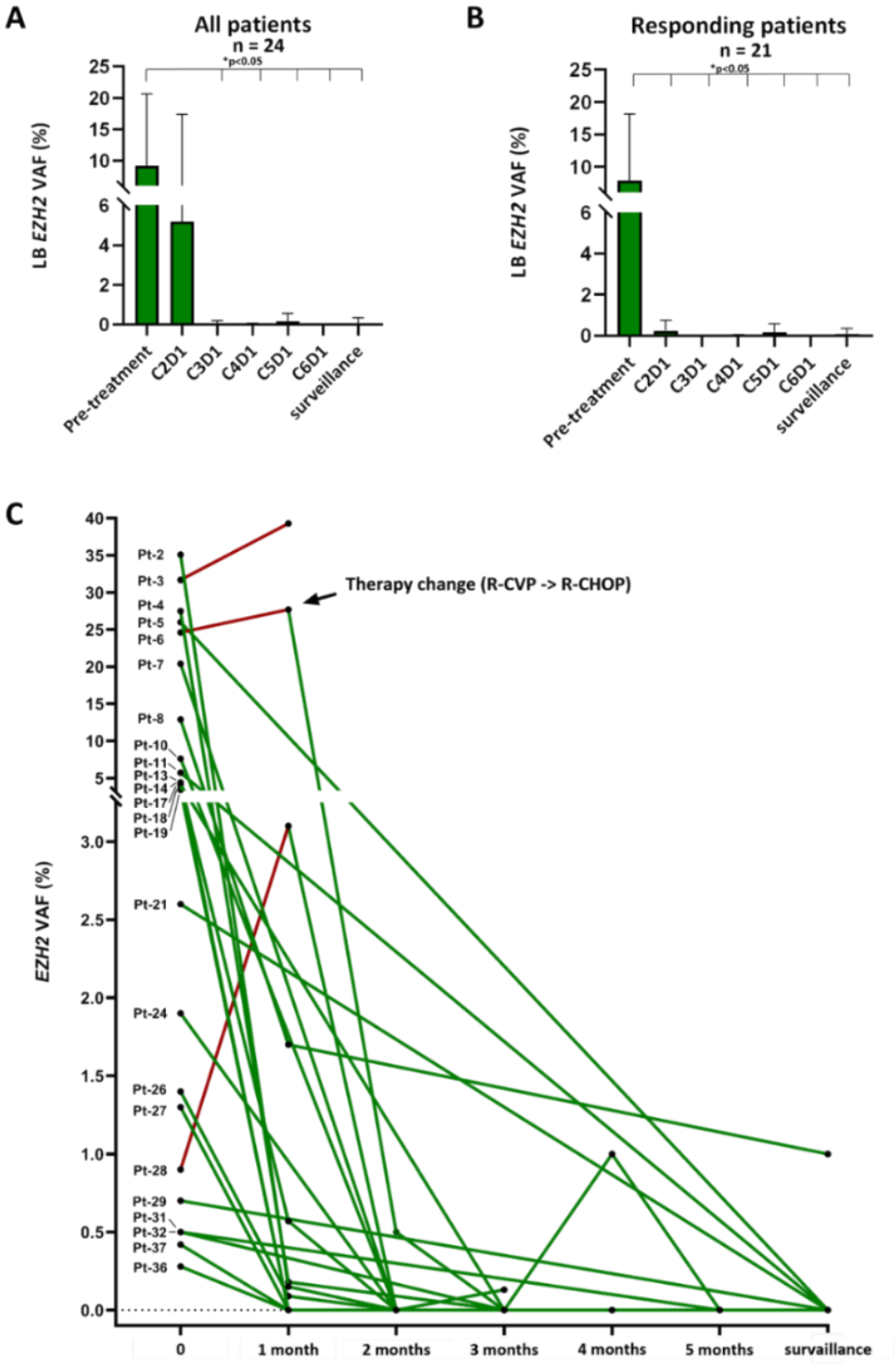

Figure 15. *EZH2 mutation analysis in longitudinally collected follow-up liquid biopsy samples.* ***A****: Mean EZH2 variant allele frequencies (VAF) before each treatment cycle in all patients.* ***B****: Mean EZH2 variant allele frequencies (VAF) before each treatment cycle in patients responding to therapy.* ***C****: Spider plot showing alterations in liquid biopsy (LB) EZH2 VAFs in response to therapy in patients with follow-up liquid biopsy samples. X axis shows elapsed time in months from treatment initiation. Patients without clinical response are labelled with red. C1D1: cycle 1 day 1. C2D1: cycle 2 day 1. C3D1: cycle 3 day 1. C4D1: cycle 4 day 1. C5D1: cycle 5 day 1. C6D1: cycle 6 day 1. R-CHOP: rituximab, cyclophosphamide, doxorubicin, vincristine, prednisone. R-CVP: rituximab, cyclophosphamide, vincristine, prednisolone.*

The excellent clinical response was promptly mirrored by LB analysis in Pt-7, where both *EZH2* mutations quickly eliminated after only one cycle of ICT treatment, five months prior to the PET/CT examination, which eventually confirmed the complete metabolic response (Figure 12A). On the other hand, Pt-6, who was first treated with R-CVP at the time of relapse, showed no improvement in clinical symptoms after two cycles. The treatment was then eventually intensified to R-CHOP and a prompt response was registered clinically and molecularly as well (Figure 16A). We observed fluctuant mutant *EZH2* ctDNA kinetics in Pt-3 at the time of relapse, who was treated with intensified regimens with the intent of ASCT. Initially, prompt molecular responses were detected in the LB compartment at day 8 after R-DHAP and R-IGEV (rituximab, ifosfamide, gemcitabine, vinorelbine) regimens, however, the disease proved to be refractory to both and to all subsequent salvage therapies (Figure 16B). Surveillance LB sampling provided proof-of-concept for early relapse detection in the case of Pt-118, who experienced *EZH2* mutant relapse one year after rituximab monotherapy, where *EZH2* p.Y646N mutation was detected in the LB specimen. Interestingly, the same *EZH2* p.Y646N with low VAF was detected six months before the clinical relapse in a surveillance LB sample (Figure 16C).

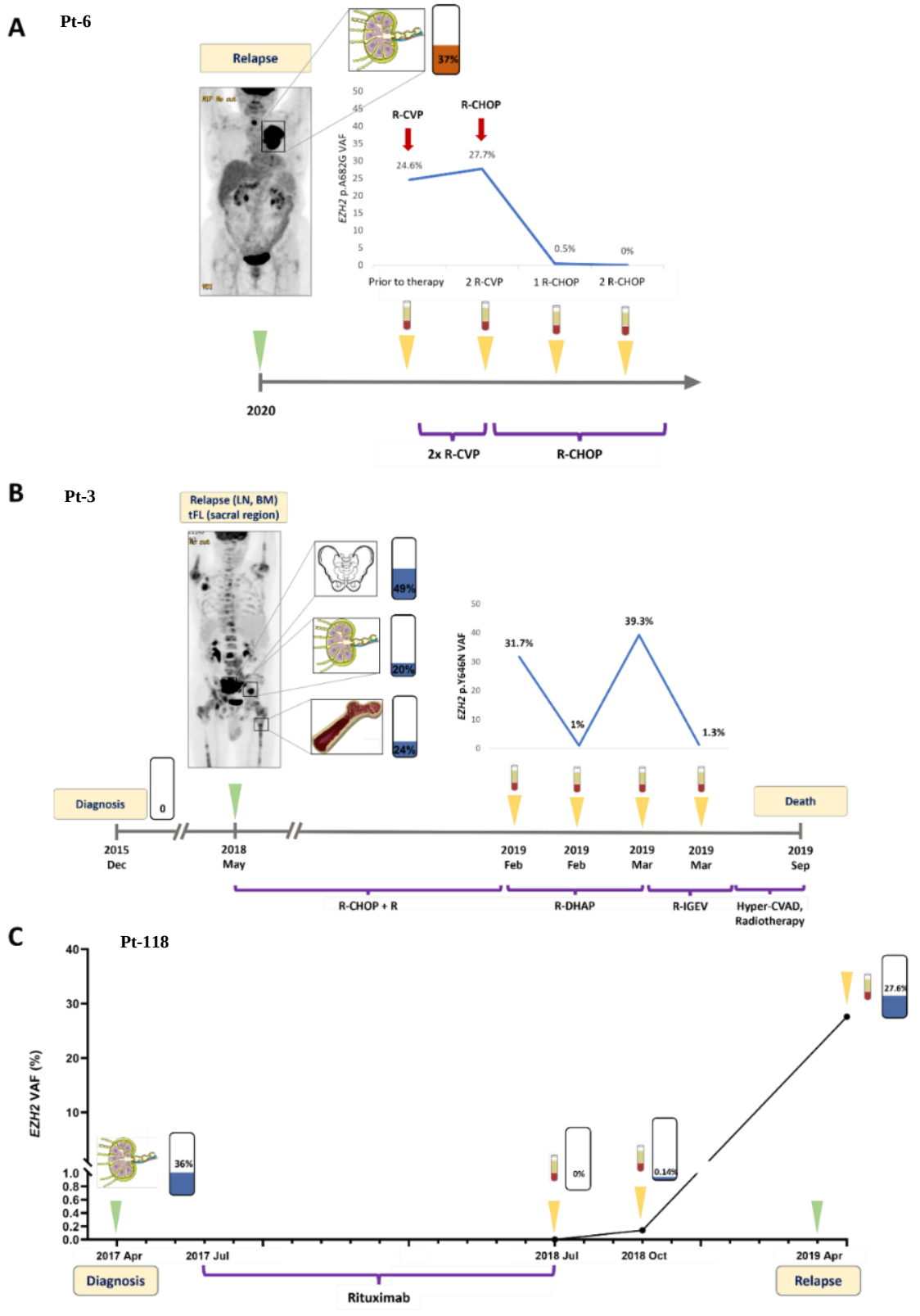

***Figure 16. A**: Illustration of temporal changes in EZH2 variant allele frequencies (VAF) in response to therapy in the case of Pt-6. **B**: Detailed illustration of treatment monitoring in Pt-3. EZH2 p.Y646N mutations were found in three sites at relapse. ctDNA EZH2*

p.Y646N allele frequencies fluctuated in parallel with treatment efficacy and refractoriness. Failure to eliminate EZH2 mutations from the plasma indicated poor prognosis. ***C****: Illustration of clonal expansion of the EZH2 mutant clone in the case of Pt-118. The patient was treated with upfront rituximab monotherapy and subsequently reached complete remission. Liquid biopsy (LB) sample collected at this timepoint was found to be EZH2 wild-type. Ten months later, the patient relapsed to an EZH2 mutant follicular lymphoma, at this timepoint the EZH2 mutation could be detected in the peripheral blood with a relatively high VAF. When analyzed retrospectively, the same mutation could be detected in the LB specimen seven months prior to relapse with low VAF. Numbers in the rectangles represent the VAF of the mutation. BM: bone marrow. Hyper-CVAD: Course A: cyclophosphamide, vincristine, doxorubicin, dexamethasone. Course B: methotrexate, cytarabine. LN: lymph node. R-CHOP: rituximab, cyclophosphamide, doxorubicin, vincristine, prednisone. R-CVP: rituximab, cyclophosphamide, vincristine, prednisolone. R-DHAP: rituximab, dexamethasone, high-dose cytarabine, cisplatin. R-IGEV: rituximab, ifosfamide, gemcitabine, vinorelbine. tFL: transformed follicular lymphoma.*

IV.7. Comparison of *EZH2* mutation analysis in LB and PBMNC specimens

We tested the *EZH2* mutation status of PBMNC samples of patients whose paired LB sample carried an *EZH2* mutation. Fifty-five paired PBMNC and LB samples were available for analysis with only 17/55 (31%) PBMNC samples carrying the *EZH2* mutation detected in the corresponding LB sample. Interrogating these 17 samples, *EZH2* VAF was significantly higher in the LB samples compared to the corresponding PBMNC samples (mean VAF: 5.7% vs 0.05%, Wilcoxon signed-rank test, $p<0.0001$) (Figure 17).

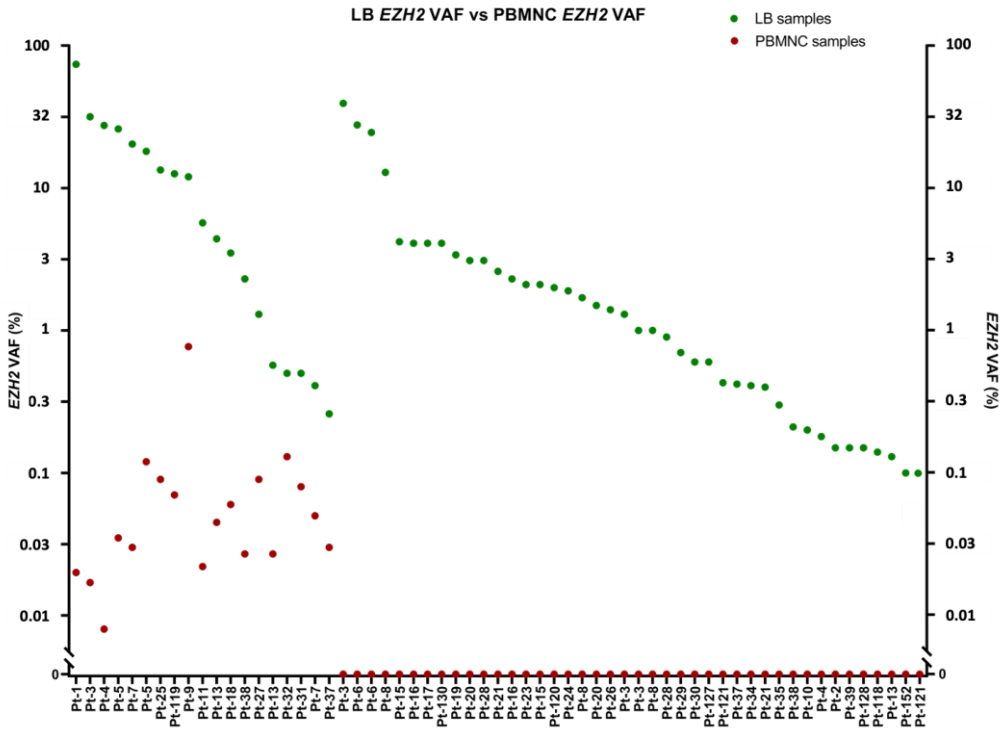

Figure 17. *Comparison of EZH2 variant allele frequencies (VAF) between liquid biopsy (LB) and peripheral blood mononuclear cell samples (PBMNC). VAFs are displayed on a log2 scale. Original VAFs (LB VAF range: 0.1-74.0%, PBMNC VAF range: 0.008-0.77%) were multiplied by 1000 (to avoid negative and zero values), then transformed to a log2 scale. Values are sorted from left to right in a descending order based on LB VAFs. Cases with detectable EZH2 mutations in the PBMNC sample are clustered to the left.*

V. Discussion

In my PhD work, we developed a unique, novel, multiplex ddPCR-based approach for the cost-effective, reliable, and sensitive detection of *EZH2* mutations from TB and LB samples of patients with FL (57). Owing to the substantial spatial and temporal heterogeneity of the disease, we detected these mutations in a significantly higher proportion of the patients, which finding may increase the number of FL cases, who most likely would benefit from recently approved selective EZH2 inhibitor treatment in the near future.

V.1. Development of the multiplex ddPCR assay

Minimal invasive ddPCR-based *EZH2* analysis is mainly restricted by the usually low cfDNA material in the plasma and the multiple single nucleotide variations presented in three loci in exons 16 and 18. In this study, we designed a novel multiplex droplet digital PCR approach to simultaneously detect multiple *EZH2* mutations in the peripheral blood, reducing the number of PCR reactions needed and consequently the required cfDNA amount. The multiplexing approach also reduces the hands-on time; hence one needs to perform only two PCR reactions, instead of seven individual amplifications. Previously, several groups have shown that multiple targets can be investigated with ddPCR in the same amplification (55, 56, 58). Our multiplex ddPCR assay uses different allele-specific hydrolysis probe concentrations, therefore different targets labelled with the same fluorophore can be distinguished in a two-channel system. In a dilution series, we demonstrated that multiplexing does not affect the LOD in the majority of the targets compared to single PCR. Multiplexing only affected the analytical sensitivity of two hotspots (p.Y646H, p.A692V), but the measured LOD for these targets are still below 0.1%. We also showed that the multiplexing approach does not influence the calculated VAF, permitting this method to be an alternative of classical single target ddPCR experiments.

Besides the detection of *EZH2* mutations (57, 59), ddPCR was previously shown to be useful in detecting other mutations characteristic of NHLs, including *MYD88*, *B-RAF*, *BTK*, *NOTCH1*, and *TP53* (60, 61). As for other small molecular inhibitors, such as gefitinib, ibrutinib, or venetoclax, it can be anticipated that resistance mutations to tazemetostat will occur in the *EZH2* gene, most probably in the D1 domain (62). Our

multiplex PCR assay will potentially be eligible for expansion towards incorporating future resistance mutation-specific probes as well, predicting the loss of tazemetostat efficacy with valuable clinical lead time.

The real-time PCR-based cobas® *EZH2* Mutation Test (Roche, Switzerland) is available in the United States as a companion diagnostic test for the analysis of FFPE tissues. With this test up to 30 samples can be tested in a 96-well plate, here the *EZH2* mutation status is determined using 3 reactions for each sample. The test requires at least 50 ng DNA input per reaction, it only reports qualitative results (no VAF is reported) and it is not able to distinguish all of the analyzed *EZH2* mutations (p.Y646H, p.Y646S and p.Y646C are reported as p.Y646X). The LOD of the cobas® test ranges between 1-5% mutation level. On the contrary, our multiplex ddPCR-based method distinguishes all *EZH2* hotspots using only two PCR reactions, it requires only 25 ng DNA per reaction, and it yields quantitative results (VAF) as well. With our system up to 43 samples can be analyzed in a 96-well plate and the LOD for each target proved to be below 0.1%, enabling this technique to be used in LB-based experiments.

Although, ddPCR offers a quick, sensitive and a relatively cheap approach for targeted mutation detection, it is a low-throughput method, therefore approaches, like multiplexing, which can increase the detected targets in a single amplification are needed. Multiple targets in cell-free DNA can be investigated with NGS-based methods as well, however the cost is substantially higher, and the interpretation requires complex bioinformatic approaches (63).

V.2. Analysis of *EZH2* mutations in classical TB and LB samples

EZH2 gain of function hotspot mutations in exons 16 and 18 were discovered by Morin et al. (23, 64). Subsequently, *EZH2* mutation frequency in FL was described to be 12% by Sanger sequencing (65). More sensitive NGS-based methods later revealed that 20-27% of FL patients harbor these mutations (19, 22, 66). The largest published cohort of nearly 600 patients so far has confirmed these results (67). However, these studies relied on single-site tissue biopsies obtained at single timepoints which may not represent the indolent systematic disease. Here, we report *EZH2* mutations in 38.4% of the 117 paired TB and LB samples with a mutation frequency of 42.1% in the whole cohort of 126 FL patients. The higher mutation frequency in our cohort can be explained by two reasons:

i), spatial heterogeneity in clonal processes leading to different clonal composition, both within one tumor site and between different tumor sites and ii), the acquisition of *EZH2* mutations during the disease course as a result of temporal evolution.

The first explanation of the higher *EZH2* mutation prevalence documented in this study is the phenomenon of spatial heterogeneity. Here, we report 9 patients where *EZH2* mutations were exclusively detected in the plasma specimen. These patients harbored a median 5 (range 2-10), metabolically active, unbiopsied tumor regions by PET/CT, which may indeed represent the origin of the *EZH2* mutant ctDNA fragments detected in LB samples. This finding underlines the value of LB in capturing genetic information blinded to random single-site biopsies. Germinal center B-cell lymphomas are characterized by a profound spatial heterogeneity proved in studies investigating multisite tissue biopsies (29, 68). Analyzing paired LB and TB samples, 8-50% of all detected mutations were found only in the ctDNA compartment in studies investigating HLs or DLBCLs (69-72). Scrutinizing immunoglobulin gene rearrangement in FL, Sarkozy et al. found that 7% of all detected rearrangements were recovered only from the plasma specimen (73). In a recent study using targeted sequencing, 8% of all mutations were exclusively found only in the LB specimen of FL patients (74). In our study, interrogating only a single gene with high sensitivity in patients with paired TB-LB biopsies, the proportion of patients where *EZH2* mutation was exclusively identified in the blood plasma was 7.7%. Moreover, 26.4% (14/53) of all *EZH2* mutations were exclusively found in the LB specimen, most likely as a result of spatial heterogeneity. The proportion of patients with spatial heterogeneity phenomenon may be even higher when using a larger gene panel with NGS. These result underlines the importance of LB-based investigation in FL.

Second, supporting the consideration of temporal evolution in the evaluation of *EZH2* mutation status, our cohort contained 39 FL patients with paired *EZH2* analysis at diagnosis and relapse, where we report *EZH2* mutation status class switch (including both gain and loss) in 35.9% of cases. This data demonstrates that *EZH2* mutation status can dynamically change throughout the disease course, may exhibit significant clonal tiding, therefore *EZH2* mutation frequency in FL can be underestimated if not analyzed temporally before each therapy line. In this subgroup of patients, the *EZH2* mutation frequency was found to be 51.3% from samples collected before treatment, which is even higher proportion compared to what we detected in the entire cohort, moreover, the

follow-up period for 30 patients at the time of data cut-off was below six months. Taken together, regarding that the *EZH2* mutation status can appear exclusively at the time of disease progression or relapse, one can anticipate that the prevalence of *EZH2* mutations is even higher if the mutation is analyzed throughout the disease course.

Of note, we could not detect *EZH2* mutations in the LB specimen of six patients, albeit the paired TB sample proved to harbor the mutation. This observation is in line with the reported result of Camus et al. where five HL patients in a cohort of 94 had WT LB test although their paired TB revealed an *XPO1* p.E571K mutation (75). In the study of Fernández-Miranda et al., 25% of all mutations were only found in the TB specimen of FL patients (74), whereas in our study, 17% of all *EZH2* mutations were not detected in the peripheral blood. In detail, Pt-44 carried a subclonal mutation (1.51%) in the TB sample, most likely explaining the *EZH2* WT status in the LB sample, however, the discordant mutation status could not be explained by histological, clinical, and radiological data in the other five patients. Owing to these outlying results, the negative predictive value of our LB-based approach is 92% and the specificity is 89%. These results show that LB analysis alone may not always be sufficient in detecting disease-specific biomarkers. However, one has to emphasize that the statistical sensitivity and the NPV of the LB-based mutation analysis were found to be superior compared to TB-based analysis (87% vs 80% and 92% vs 89%, respectively). According to our results, the best sensitivity for *EZH2* mutation analysis can be achieved with the parallel investigation of TB and LB samples.

Tazemetostat, a novel, orally active inhibitor of *EZH2* was recently approved in the US for R/R *EZH2* mutant FL patients who received at least two prior systemic therapy and for patients who have no satisfactory alternative treatment options, regardless of their *EZH2* mutation status (27). The approval was based on a phase II, multicenter, single-arm clinical study, where the objective response rate to single-agent tazemetostat in a pretreated cohort was found to be 69% and 35% in *EZH2* mutant and wild-type FL patients, respectively. In a preliminary communication of this study, the authors highlighted that the presence of *EZH2* mutation was the only predictor of response in both TB and LB in patients with FL (76). It is also noteworthy, that around one-third of patients with wild-type *EZH2* also showed a response to the treatment. The substantially higher *EZH2* mutation frequency in this study, in addition to genotypic (gene amplification),

gene expression-based alterations, and microenvironmental factors, may also explain at least a proportion of the unanticipated response to tazemetostat monotherapy in 35% of the *EZH2* wild-type cohort of the phase II study.

V.3. Correlation between *EZH2* mutation status and allele burden and clinical variables

We found a statistically significant correlation between histological grade and *EZH2* mutation status: *EZH2* mutations were more common in the high-grade group (3B/transformed FL, 53%) compared to classical FL (grade 1/2/3A, 28%). This finding is in line with the result by Bouska et al., reporting an *EZH2* mutation frequency of 50% in paired FL - transformed FL samples (26). Martínez-Laperche et al. also found an association between *EZH2* mutation status and more aggressive FL histology (77). Of note, other studies did not find an increase in the *EZH2* mutation frequency in transformed FL (19, 20, 78). In our cohort, *EZH2* VAF was also higher in histologically more aggressive diseases, which may be explained by the more abundant immune cell infiltration in FL compared to aggressive lymphomas (DLBCL) (79).

Huet et al. reported an inverse correlation between *EZH2* alterations (mutation and amplification) and B-symptoms and rate of BM infiltration in FL (80). Here, we also observed an association between *EZH2* mutant FL and lack of BM infiltration. When analyzing paired lymph node and BM biopsies we found that the *EZH2* wild-type FL clone may be more prone to infiltrate the BM compared to the *EZH2* mutant clone. These findings raise the idea that the lack of *EZH2* mutation in FL may be a biomarker indicating an increased risk of BM infiltration, however, this needs to be confirmed in larger cohorts. In contrast with the observations by Huet et al. (80), we detected a significant association between the presence of *EZH2* mutations and B-symptoms.

Tumor burden is an established prognostic factor in lymphomas, therefore methods accurately measuring this parameter are of great clinical need. The increased metabolic activity, characteristic of aggressive lymphomas is usually accompanied by increased ctDNA excretion to the blood (81). In line with this, here we report a trend between LB *EZH2* VAF levels and more aggressive histology. In DLBCL and HL, it is well documented that pre-treatment ctDNA levels independently mirror distinct parameters that indicate tumor burden (international prognostic index, LDH level, stage, and total

metabolic tumor volume (TMTV)) (70, 72, 82, 83). In FL, TMTV is the only parameter that has been independently linked to LB ctDNA abundance (73, 84, 85). In the study of Sarkozy et al., no correlation was found between ctDNA levels determined by immunoglobulin gene rearrangement, and FLIPI score, BM infiltration, or bulky disease (73). In a recent study, using a 78-gene targeted sequencing panel, baseline ctDNA levels correlated with FLIPI score, extranodal involvement, and elevated LDH, although no significant differences were observed between stage categories (74). We did not find a significant correlation between LB *EZH2* VAF levels and basic clinical parameters, although we found a trend with clinical stage, FLIPI, LDH levels, presence of extranodal involvement and PET/CT determined SUV max value, where the more aggressive clinical factors were always accompanied by higher mean LB *EH2* VAF levels. The non-significant associations may be explained by the relatively small number of investigated patients with *EZH2* mutation in the plasma (n=43), which sample size may not be enough to uncover statistically significant associations in an indolent lymphoma. Moreover, investigation of a single gene may not accurately represent the total amount of ctDNA molecules in the plasma in a genetically diverse disease, such as FL (the sole investigation of the *EZH2* gene does not inform about the *EZH2* wild-type fraction of the tumor). Importantly, in one patient (Pt-1), an extremely high VAF indicated high tumor burden and very poor prognosis.

V.4. LB-based treatment monitoring in FL

Undetectable ctDNA or at least a 100-fold reduction in ctDNA levels after 2 cycles of therapy indicates excellent treatment response and outcome in DLBCL, HL, and mantle cell lymphoma (MCL) as well (72, 86-88). Here we found a significant drop (>100-fold) in the *EZH2* levels after two cycles of immunochemotherapy comparing pre-treatment and C3D1 levels. No statistical difference was observed between pre-treatment and C2D1 timepoints regarding all patients, however, statistical difference was detected between pre-treatment and C2D1 levels when restricting the analysis to responding patients, indicating that investigation of LB samples may mirror early therapeutic response in FL and dynamic monitoring of ctDNA levels might have similar clinical value as in DLBCL or in HL. In line with this, Fernández-Miranda et al. recently showed that responding patients have a more rapid decrease in their ctDNA level (74). The previously presented cases of Pt-3, Pt-6 and Pt-7 demonstrate that monitoring of the early kinetics of ctDNA

offers a real-time, radiation-free disease monitoring alternative to imaging-based methods in FL as well. The case of Pt-6 and Pt-7 also show that failure to eliminate or significantly decrease the mutant allele burden in the LB compartment after even one complete therapy cycle indicates lack of treatment response.

During surveillance, in the majority of DLBCL and MCL cases, signs of lymphoma recurrence can be detected with a 3–7-month lead time with LB analysis (83, 88, 89). To the best of our knowledge, no data is available in the context of minimal residual disease detection using ctDNA in FL. Here, we demonstrate an FL case (Pt-118) where mutant *EZH2* ctDNA fragments could be detected during surveillance, six months prior to the clinical relapse, harboring an identical *EZH2* mutation within the relapse sample. This case indicates that LB-based monitoring of FL may be valuable in predicting future relapses.

V.5. *EZH2* mutation detection analysis comparing the cellular and acellular component of the blood

The majority of the studies in the last three decades published about the minimal-invasive detection and monitoring of FL focused on the interrogation of *BCL2*/*IGH* translocation or the clonal V(D)J rearrangements from PBMNCs (63, 90, 91). To date, no one has directly compared the value of the cellular and acellular compartment of the peripheral blood in FL for molecular analysis. Here, we show that mutant *EZH2* DNA fragments can be more sensitively detected from ctDNA compared to PBMNCs. In our cohort, the majority of PBMNC samples with paired mutant LB samples lacked *EZH2* mutation, moreover, the *EZH2* VAF values in *EZH2* mutant PBMNCs were substantially lower compared to the corresponding LB samples. This supports the theory that ctDNA may be more reliable in detecting traits of the disease compared to PBMNC-based methods in FL.

VI. Conclusions

1) We developed a unique multiplex ddPCR assay, which can cost-effectively detect all the seven *EZH2* hotspot mutations in FL using only two PCR reactions.
2) In an unselected cohort of Hungarian FL patients, the *EZH2* mutation frequency proved to be 42.1%, higher than the previously published literature data (25%). The higher mutation frequency in FL may further expand the subset of patients who would most likely benefit from the recently approved targeted therapy.
3) Spatial heterogeneity is frequent in FL and contributes to the higher *EZH2* mutation detection rate in this study. *EZH2* mutations are also directly detectable from LB samples. The sensitivity and NPV of the LB-based *EZH2* mutation detection analysis slightly outperforms the TB-based one (87%, 92% vs. 80%, 89%).
4) *EZH2* mutations represent a dynamic biomarker in FL, with the mutation potentially changing throughout the disease course.
5) Mutant *EZH2* status is associated with more aggressive histology, presence of B-symptoms and lack of BM infiltration. Mutant *EZH2* allele burden showed a correlation trend towards higher clinical stage, FLIPI score, LDH levels, SUV max value, TB *EZH2* VAF level, more aggressive TB histology and presence of extranodal involvement. These results indicate that overall ctDNA levels in FL may mirror tumor burden.
6) ctDNA kinetics indicate treatment responses in FL.
7) The acellular component of the blood (ctDNA) is more reliable sample source for DNA-based biomarker analysis in FL than the cellular part.

VII. Summary

Follicular lymphoma is the most common indolent non-Hodgkin lymphoma. Despite the usual indolent nature and the modern immunochemotherapeutic regimens, the disease is still incurable, and frequent relapses and high-grade transformation to a more aggressive lymphoma can characterize the disease. Research efforts in the last decade elucidated the genetic background of the disease, most strikingly, they revealed that the epigenetic machinery is affected in all cases. Activating mutations in the epigenetic regulator gene *EZH2* are present in around 25% of the cases. The gain of function nature of these mutations proved to be an attractive therapeutic target, and consequently the selective EZH2 inhibitor has been approved in the United States. The presence of *EZH2* mutations is a predictive biomarker of the therapy, therefore techniques able to sensitively detect these alterations are needed.

FL is also characterized by a profound spatial heterogeneity, which means that distinct disease sites can differ from each other morphologically and molecularly. The minimal invasive investigation of circulating tumor DNA in the blood is a promising method for analyzing spatial heterogeneity hence it represents the systematic disease.

In my PhD work we developed a unique multiplex ddPCR assay which can cost-effectively detect all of the seven *EZH2* mutation types using only two PCR reactions.

In the framework of a nation-wide collaboration, we collected liquid and tissue biopsy samples from 126 FL patients, to test the detectability of *EZH2* mutations in both sample types and to determine the frequency of the mutations.

We found that *EZH2* mutations are more frequent in FL if both, LB, and TB samples are parallelly tested, as a result of spatial heterogeneity. We also showed that *EZH2* mutations are an unstable biomarker, hence these mutations can appear exclusively at the time of relapse.

We also found that ctDNA abundance in the blood may mirror tumor burden in FL, since we have seen a trend between LB *EZH2* VAFs and histological grade and several clinical parameters. In a subset of patients with follow-up LB samples, we showed that ctDNA kinetics reflects treatment responses; we have seen rapid elimination of the mutations in responding patients, on the contrary *EZH2* VAFs did not decreased in non-responders.

VIII. References

1. Ziegler A, Koch A, Krockenberger K, Grosshennig A. Personalized medicine using DNA biomarkers: a review. Hum Genet. 2012;131(10):1627-38.

2. Corcoran RB, Chabner BA. Application of Cell-free DNA Analysis to Cancer Treatment. N Engl J Med. 2018;379(18):1754-65.

3. Nagy Á, Lévay L, Zajta E, Gergő P. A folyadékbiopszia nyújtotta lehetõségek a szolid daganatok molekuláris diagnosztikájában. Orvosképzés. 2021;46(3):12.

4. Nagy Á, Bátai B, Kiss L, Marx A, Pinczés LI, Papp G, Kacskovics I, Alpár D, Bodor C. Folyadékbiopszia-vizsgálatok alkalmazási lehetőségei az onkohematológiában. Hematológia–Transzfuziológia. 2020;53(3):144-56.

5. Kuppers R. Mechanisms of B-cell lymphoma pathogenesis. Nat Rev Cancer. 2005;5(4):251-62.

6. Chi X, Li Y, Qiu X. V(D)J recombination, somatic hypermutation and class switch recombination of immunoglobulins: mechanism and regulation. Immunology. 2020;160(3):233-47.

7. Alaggio R, Amador C, Anagnostopoulos I, Attygalle AD, Araujo IBO, Berti E, Bhagat G, Borges AM, Boyer D, Calaminici M, Chadburn A, Chan JKC, Cheuk W, Chng WJ, Choi JK, Chuang SS, Coupland SE, Czader M, Dave SS, de Jong D, Du MQ, Elenitoba-Johnson KS, Ferry J, Geyer J, Gratzinger D, Guitart J, Gujral S, Harris M, Harrison CJ, Hartmann S, Hochhaus A, Jansen PM, Karube K, Kempf W, Khoury J, Kimura H, Klapper W, Kovach AE, Kumar S, Lazar AJ, Lazzi S, Leoncini L, Leung N, Leventaki V, Li XQ, Lim MS, Liu WP, Louissaint A, Jr., Marcogliese A, Medeiros LJ, Michal M, Miranda RN, Mitteldorf C, Montes-Moreno S, Morice W, Nardi V, Naresh KN, Natkunam Y, Ng SB, Oschlies I, Ott G, Parrens M, Pulitzer M, Rajkumar SV, Rawstron AC, Rech K, Rosenwald A, Said J, Sarkozy C, Sayed S, Saygin C, Schuh A, Sewell W, Siebert R, Sohani AR, Tooze R, Traverse-Glehen A, Vega F, Vergier B, Wechalekar AD, Wood B, Xerri L, Xiao W. The 5th edition of the World Health Organization Classification of Haematolymphoid Tumours: Lymphoid Neoplasms. Leukemia. 2022;36(7):1720-48.

8. Carbone A, Roulland S, Gloghini A, Younes A, von Keudell G, Lopez-Guillermo A, Fitzgibbon J. Follicular lymphoma. Nat Rev Dis Primers. 2019;5(1):83.

9. Teras LR, DeSantis CE, Cerhan JR, Morton LM, Jemal A, Flowers CR. 2016 US lymphoid malignancy statistics by World Health Organization subtypes. CA Cancer J Clin. 2016;66(6):443-59.

10. Maurer MJ, Ghesquieres H, Jais JP, Witzig TE, Haioun C, Thompson CA, Delarue R, Micallef IN, Peyrade F, Macon WR, Jo Molina T, Ketterer N, Syrbu SI, Fitoussi O, Kurtin PJ, Allmer C, Nicolas-Virelizier E, Slager SL, Habermann TM, Link BK, Salles G, Tilly H, Cerhan JR. Event-free survival at 24 months is a robust end point for disease-related outcome in diffuse large B-cell lymphoma treated with immunochemotherapy. J Clin Oncol. 2014;32(10):1066-73.

11. Link BK, Maurer MJ, Nowakowski GS, Ansell SM, Macon WR, Syrbu SI, Slager SL, Thompson CA, Inwards DJ, Johnston PB, Colgan JP, Witzig TE, Habermann TM, Cerhan JR. Rates and outcomes of follicular lymphoma transformation in the immunochemotherapy era: a report from the University of Iowa/MayoClinic Specialized Program of Research Excellence Molecular Epidemiology Resource. J Clin Oncol. 2013;31(26):3272-8.

12. Tsujimoto Y, Cossman J, Jaffe E, Croce CM. Involvement of the bcl-2 gene in human follicular lymphoma. Science. 1985;228(4706):1440-3.

13. Roulland S, Faroudi M, Mamessier E, Sungalee S, Salles G, Nadel B. Early steps of follicular lymphoma pathogenesis. Adv Immunol. 2011;111:1-46.

14. Roulland S, Kelly RS, Morgado E, Sungalee S, Solal-Celigny P, Colombat P, Jouve N, Palli D, Pala V, Tumino R, Panico S, Sacerdote C, Quiros JR, Gonzales CA, Sanchez MJ, Dorronsoro M, Navarro C, Barricarte A, Tjonneland A, Olsen A, Overvad K, Canzian F, Kaaks R, Boeing H, Drogan D, Nieters A, Clavel-Chapelon F, Trichopoulou A, Trichopoulos D, Lagiou P, Bueno-de-Mesquita HB, Peeters PH, Vermeulen R, Hallmans G, Melin B, Borgquist S, Carlson J, Lund E, Weiderpass E, Khaw KT, Wareham N, Key TJ, Travis RC, Ferrari P, Romieu I, Riboli E, Salles G, Vineis P, Nadel B. t(14;18) Translocation: A predictive blood biomarker for follicular lymphoma. J Clin Oncol. 2014;32(13):1347-55.

15. Schuler F, Dolken L, Hirt C, Kiefer T, Berg T, Fusch G, Weitmann K, Hoffmann W, Fusch C, Janz S, Rabkin CS, Dolken G. Prevalence and frequency of circulating t(14;18)-MBR translocation carrying cells in healthy individuals. Int J Cancer. 2009;124(4):958-63.

16. Sungalee S, Mamessier E, Morgado E, Gregoire E, Brohawn PZ, Morehouse CA, Jouve N, Monvoisin C, Menard C, Debroas G, Faroudi M, Mechin V, Navarro JM, Drevet C, Eberle FC, Chasson L, Baudimont F, Mancini SJ, Tellier J, Picquenot JM, Kelly R, Vineis P, Ruminy P, Chetaille B, Jaffe ES, Schiff C, Hardwigsen J, Tice DA, Higgs BW, Tarte K, Nadel B, Roulland S. Germinal center reentries of BCL2-overexpressing B cells drive follicular lymphoma progression. J Clin Invest. 2014;124(12):5337-51.

17. Korfi K, Ali S, Heward JA, Fitzgibbon J. Follicular lymphoma, a B cell malignancy addicted to epigenetic mutations. Epigenetics. 2017;12(5):370-7.

18. Kridel R, Chan FC, Mottok A, Boyle M, Farinha P, Tan K, Meissner B, Bashashati A, McPherson A, Roth A, Shumansky K, Yap D, Ben-Neriah S, Rosner J, Smith MA, Nielsen C, Gine E, Telenius A, Ennishi D, Mungall A, Moore R, Morin RD, Johnson NA, Sehn LH, Tousseyn T, Dogan A, Connors JM, Scott DW, Steidl C, Marra MA, Gascoyne RD, Shah SP. Histological Transformation and Progression in Follicular Lymphoma: A Clonal Evolution Study. PLoS Med. 2016;13(12):e1002197.

19. Okosun J, Bodor C, Wang J, Araf S, Yang CY, Pan C, Boller S, Cittaro D, Bozek M, Iqbal S, Matthews J, Wrench D, Marzec J, Tawana K, Popov N, O'Riain C, O'Shea D, Carlotti E, Davies A, Lawrie CH, Matolcsy A, Calaminici M, Norton A, Byers RJ, Mein C, Stupka E, Lister TA, Lenz G, Montoto S, Gribben JG, Fan Y, Grosschedl R, Chelala C, Fitzgibbon J. Integrated genomic analysis identifies recurrent mutations and evolution patterns driving the initiation and progression of follicular lymphoma. Nat Genet. 2014;46(2):176-81.

20. Pasqualucci L, Khiabanian H, Fangazio M, Vasishtha M, Messina M, Holmes AB, Ouillette P, Trifonov V, Rossi D, Tabbo F, Ponzoni M, Chadburn A, Murty VV, Bhagat G, Gaidano G, Inghirami G, Malek SN, Rabadan R, Dalla-Favera R. Genetics of follicular lymphoma transformation. Cell Rep. 2014;6(1):130-40.

21. Okosun J, Wolfson RL, Wang J, Araf S, Wilkins L, Castellano BM, Escudero-Ibarz L, Al Seraihi AF, Richter J, Bernhart SH, Efeyan A, Iqbal S, Matthews J, Clear A, Guerra-Assuncao JA, Bodor C, Quentmeier H, Mansbridge C, Johnson P, Davies A, Strefford JC, Packham G, Barrans S, Jack A, Du MQ, Calaminici M, Lister TA, Auer R, Montoto S, Gribben JG, Siebert R, Chelala C, Zoncu R, Sabatini DM, Fitzgibbon J. Recurrent mTORC1-activating RRAGC mutations in follicular lymphoma. Nat Genet. 2016;48(2):183-8.

22. Bodor C, Grossmann V, Popov N, Okosun J, O'Riain C, Tan K, Marzec J, Araf S, Wang J, Lee AM, Clear A, Montoto S, Matthews J, Iqbal S, Rajnai H, Rosenwald A, Ott G, Campo E, Rimsza LM, Smeland EB, Chan WC, Braziel RM, Staudt LM, Wright G, Lister TA, Elemento O, Hills R, Gribben JG, Chelala C, Matolcsy A, Kohlmann A, Haferlach T, Gascoyne RD, Fitzgibbon J. EZH2 mutations are frequent and represent an early event in follicular lymphoma. Blood. 2013;122(18):3165-8.

23. Morin RD, Johnson NA, Severson TM, Mungall AJ, An J, Goya R, Paul JE, Boyle M, Woolcock BW, Kuchenbauer F, Yap D, Humphries RK, Griffith OL, Shah S, Zhu H, Kimbara M, Shashkin P, Charlot JF, Tcherpakov M, Corbett R, Tam A, Varhol R, Smailus D, Moksa M, Zhao Y, Delaney A, Qian H, Birol I, Schein J, Moore R, Holt R, Horsman DE, Connors JM, Jones S, Aparicio S, Hirst M, Gascoyne RD, Marra MA. Somatic mutations altering EZH2 (Tyr641) in follicular and diffuse large B-cell lymphomas of germinal-center origin. Nat Genet. 2010;42(2):181-5.

24. Vire E, Brenner C, Deplus R, Blanchon L, Fraga M, Didelot C, Morey L, Van Eynde A, Bernard D, Vanderwinden JM, Bollen M, Esteller M, Di Croce L, de Launoit Y, Fuks F. The Polycomb group protein EZH2 directly controls DNA methylation. Nature. 2006;439(7078):871-4.

25. Bátai B, Lévai D, Gaál-Weisinger J, Balogh A, Gángó A, Bodor C, Nagy N. A személyre szabott terápia új lehetősége follicularis lymphomában – Az EZH2 hiszton metil-transzferáz gátlása. Hematológia–Transzfuziológia. 2018;51(2):61-70.

26. Bouska A, Zhang W, Gong Q, Iqbal J, Scuto A, Vose J, Ludvigsen M, Fu K, Weisenburger DD, Greiner TC, Gascoyne RD, Rosenwald A, Ott G, Campo E, Rimsza LM, Delabie J, Jaffe ES, Braziel RM, Connors JM, Wu CI, Staudt LM, D'Amore F, McKeithan TW, Chan WC. Combined copy number and mutation analysis identifies oncogenic pathways associated with transformation of follicular lymphoma. Leukemia. 2017;31(1):83-91.

27. FDA granted accelerated approval to tazemetostat for follicular lymphoma. 2020.

28. Morschhauser F, Tilly H, Chaidos A, McKay P, Phillips T, Assouline S, Batlevi CL, Campbell P, Ribrag V, Damaj GL, Dickinson M, Jurczak W, Kazmierczak M, Opat S, Radford J, Schmitt A, Yang J, Whalen J, Agarwal S, Adib D, Salles G. Tazemetostat for patients with relapsed or refractory follicular lymphoma: an open-label, single-arm, multicentre, phase 2 trial. Lancet Oncol. 2020;21(11):1433-42.

29. Araf S, Wang J, Korfi K, Pangault C, Kotsiou E, Rio-Machin A, Rahim T, Heward J, Clear A, Iqbal S, Davies JK, Johnson P, Calaminici M, Montoto S, Auer R, Chelala C, Gribben JG, Graham TA, Fest T, Fitzgibbon J, Okosun J. Genomic profiling reveals spatial intra-tumor heterogeneity in follicular lymphoma. Leukemia. 2018;32(5):1261-5.

30. Haebe S, Shree T, Sathe A, Day G, Czerwinski DK, Grimes SM, Lee H, Binkley MS, Long SR, Martin B, Ji HP, Levy R. Single-cell analysis can define distinct evolution of tumor sites in follicular lymphoma. Blood. 2021;137(21):2869-80.

31. Armitage JO. Staging Non-Hodgkin Lymphoma. CA: A Cancer Journal for Clinicians. 2005;55(6):368-76.

32. Buske C, Hoster E, Dreyling M, Hasford J, Unterhalt M, Hiddemann W. The Follicular Lymphoma International Prognostic Index (FLIPI) separates high-risk from intermediate- or low-risk patients with advanced-stage follicular lymphoma treated front-line with rituximab and the combination of cyclophosphamide, doxorubicin, vincristine, and prednisone (R-CHOP) with respect to treatment outcome. Blood. 2006;108(5):1504-8.

33. Pastore A, Jurinovic V, Kridel R, Hoster E, Staiger AM, Szczepanowski M, Pott C, Kopp N, Murakami M, Horn H, Leich E, Moccia AA, Mottok A, Sunkavalli A, Van Hummelen P, Ducar M, Ennishi D, Shulha HP, Hother C, Connors JM, Sehn LH, Dreyling M, Neuberg D, Moller P, Feller AC, Hansmann ML, Stein H, Rosenwald A, Ott G, Klapper W, Unterhalt M, Hiddemann W, Gascoyne RD, Weinstock DM, Weigert O. Integration of gene mutations in risk prognostication for patients receiving first-line immunochemotherapy for follicular lymphoma: a retrospective analysis of a prospective clinical trial and validation in a population-based registry. Lancet Oncol. 2015;16(9):1111-22.

34. Advani R, Rosenberg SA, Horning SJ. Stage I and II follicular non-Hodgkin's lymphoma: long-term follow-up of no initial therapy. J Clin Oncol. 2004;22(8):1454-9.

35. Ardeshna KM, Smith P, Norton A, Hancock BW, Hoskin PJ, MacLennan KA, Marcus RE, Jelliffe A, Vaughan G, Hudson, Linch DC, British National Lymphoma I. Long-term effect of a watch and wait policy versus immediate systemic treatment for asymptomatic advanced-stage non-Hodgkin lymphoma: a randomised controlled trial. Lancet. 2003;362(9383):516-22.

36. Marcus R, Davies A, Ando K, Klapper W, Opat S, Owen C, Phillips E, Sangha R, Schlag R, Seymour JF, Townsend W, Trneny M, Wenger M, Fingerle-Rowson G, Rufibach K, Moore T, Herold M, Hiddemann W. Obinutuzumab for the First-Line Treatment of Follicular Lymphoma. N Engl J Med. 2017;377(14):1331-44.

37. McNamara C, Montoto S, Eyre TA, Ardeshna K, Burton C, Illidge T, Linton K, Rule S, Townsend W, Wong WL, McKay P. The investigation and management of follicular lymphoma. Br J Haematol. 2020;191(3):363-81.

38. Salles G, Seymour JF, Offner F, Lopez-Guillermo A, Belada D, Xerri L, Feugier P, Bouabdallah R, Catalano JV, Brice P, Caballero D, Haioun C, Pedersen LM, Delmer A, Simpson D, Leppa S, Soubeyran P, Hagenbeek A, Casasnovas O, Intragumtornchai T, Ferme C, da Silva MG, Sebban C, Lister A, Estell JA, Milone G, Sonet A, Mendila M, Coiffier B, Tilly H. Rituximab maintenance for 2 years in patients with high tumour burden follicular lymphoma responding to rituximab plus chemotherapy (PRIMA): a phase 3, randomised controlled trial. Lancet. 2011;377(9759):42-51.

39. Morschhauser F, Fowler NH, Feugier P, Bouabdallah R, Tilly H, Palomba ML, Fruchart C, Libby EN, Casasnovas RO, Flinn IW, Haioun C, Maisonneuve H, Ysebaert L, Bartlett NL, Bouabdallah K, Brice P, Ribrag V, Daguindau N, Le Gouill S, Pica GM, Martin Garcia-Sancho A, Lopez-Guillermo A, Larouche JF, Ando K, Gomes da Silva M, Andre M, Zachee P, Sehn LH, Tobinai K, Cartron G, Liu D, Wang J, Xerri L, Salles GA, Investigators RT. Rituximab plus Lenalidomide in Advanced Untreated Follicular Lymphoma. N Engl J Med. 2018;379(10):934-47.

40. Fésüs V, Nagy Á, Alpár D, Bodor C. Az adoptív sejttranszfer sikere a hematológiában: a kiméra antigénreceptorral felruházott T-sejtek. Hematológia–Transzfuziológia. 2019;52(3):178-87.

41. Metser U, Hussey D, Murphy G. Impact of (18)F-FDG PET/CT on the staging and management of follicular lymphoma. Br J Radiol. 2014;87(1042):20140360.

42. Ansell SM, Armitage JO. Positron emission tomographic scans in lymphoma: convention and controversy. Mayo Clin Proc. 2012;87(6):571-80.

43. Han HS, Escalon MP, Hsiao B, Serafini A, Lossos IS. High incidence of false-positive PET scans in patients with aggressive non-Hodgkin's lymphoma treated with rituximab-containing regimens. Ann Oncol. 2009;20(2):309-18.

44. Siravegna G, Marsoni S, Siena S, Bardelli A. Integrating liquid biopsies into the management of cancer. Nat Rev Clin Oncol. 2017;14(9):531-48.

45. Heitzer E, Haque IS, Roberts CES, Speicher MR. Current and future perspectives of liquid biopsies in genomics-driven oncology. Nat Rev Genet. 2019;20(2):71-88.

46. Mandel P, Metais P. [Nuclear Acids In Human Blood Plasma]. C R Seances Soc Biol Fil. 1948;142(3-4):241-3.

47. Kustanovich A, Schwartz R, Peretz T, Grinshpun A. Life and death of circulating cell-free DNA. Cancer Biol Ther. 2019;20(8):1057-67.

48. Bobillo S, Crespo M, Escudero L, Mayor R, Raheja P, Carpio C, Rubio-Perez C, Tazon-Vega B, Palacio C, Carabia J, Jimenez I, Nieto JC, Montoro J, Martinez-Ricarte F, Castellvi J, Simo M, Puigdefabregas L, Abrisqueta P, Bosch F, Seoane J. Cell free circulating tumor DNA in cerebrospinal fluid detects and monitors central nervous system involvement of B-cell lymphomas. Haematologica. 2021;106(2):513-21.

49. Chan HT, Chin YM, Nakamura Y, Low S-K. Clonal Hematopoiesis in Liquid Biopsy: From Biological Noise to Valuable Clinical Implications. Cancers. 2020;12(8):2277.

50. Malapelle U, Sirera R, Jantus-Lewintre E, Reclusa P, Calabuig-Farinas S, Blasco A, Pisapia P, Rolfo C, Camps C. Profile of the Roche cobas(R) EGFR mutation test v2 for non-small cell lung cancer. Expert Rev Mol Diagn. 2017;17(3):209-15.

51. Warren JD, Xiong W, Bunker AM, Vaughn CP, Furtado LV, Roberts WL, Fang JC, Samowitz WS, Heichman KA. Septin 9 methylated DNA is a sensitive and specific blood test for colorectal cancer. BMC Med. 2011;9:133.

52. Quan P-L, Sauzade M, Brouzes E. dPCR: A Technology Review. Sensors. 2018;18(4):1271.

53. Hindson CM, Chevillet JR, Briggs HA, Gallichotte EN, Ruf IK, Hindson BJ, Vessella RL, Tewari M. Absolute quantification by droplet digital PCR versus analog real-time PCR. Nat Methods. 2013;10(10):1003-5.

54. Madic J, Zocevic A, Senlis V, Fradet E, Andre B, Muller S, Dangla R, Droniou ME. Three-color crystal digital PCR. Biomol Detect Quantif. 2016;10:34-46.

55. Alcaide M, Yu S, Bushell K, Fornika D, Nielsen JS, Nelson BH, Mann KK, Assouline S, Johnson NA, Morin RD. Multiplex Droplet Digital PCR Quantification of

Recurrent Somatic Mutations in Diffuse Large B-Cell and Follicular Lymphoma. Clin Chem. 2016;62(9):1238-47.

56. Watanabe M, Kawaguchi T, Isa SI, Ando M, Tamiya A, Kubo A, Saka H, Takeo S, Adachi H, Tagawa T, Kawashima O, Yamashita M, Kataoka K, Ichinose Y, Takeuchi Y, Watanabe K, Matsumura A, Koh Y. Multiplex Ultrasensitive Genotyping of Patients with Non-Small Cell Lung Cancer for Epidermal Growth Factor Receptor (EGFR) Mutations by Means of Picodroplet Digital PCR. EBioMedicine. 2017;21:86-93.

57. Nagy A, Batai B, Kiss L, Grof S, Kiraly PA, Jona A, Demeter J, Santa H, Batai A, Pettendi P, Szendrei T, Plander M, Korosmezey G, Alizadeh H, Kajtar B, Mehes G, Krenacs L, Timar B, Csomor J, Toth E, Schneider T, Mikala G, Matolcsy A, Alpar D, Masszi A, Bodor C. Parallel testing of liquid biopsy (ctDNA) and tissue biopsy samples reveals a higher frequency of EZH2 mutations in follicular lymphoma. J Intern Med. 2023.

58. Levy CN, Hughes SM, Roychoudhury P, Amstuz C, Zhu H, Huang ML, Lehman DA, Jerome KR, Hladik F. HIV reservoir quantification by five-target multiplex droplet digital PCR. STAR Protoc. 2021;2(4):100885.

59. Nagy A, Batai B, Balogh A, Illes S, Mikala G, Nagy N, Kiss L, Kotmayer L, Matolcsy A, Alpar D, Masszi T, Masszi A, Bodor C. Quantitative Analysis and Monitoring of EZH2 Mutations Using Liquid Biopsy in Follicular Lymphoma. Genes (Basel). 2020;11(7).

60. Bodor C, Kotmayer L, Laszlo T, Takacs F, Barna G, Kiss R, Sebestyen E, Nagy T, Hegyi LL, Mikala G, Fekete S, Farkas P, Balogh A, Masszi T, Demeter J, Weisinger J, Alizadeh H, Kajtar B, Kohl Z, Szasz R, Gergely L, Gurbity Palfi T, Sulak A, Kollar B, Egyed M, Plander M, Rejto L, Szerafin L, Ilonczai P, Tamaska P, Pettendi P, Levai D, Schneider T, Sebestyen A, Csermely P, Matolcsy A, Matrai Z, Alpar D. Screening and monitoring of the BTK(C481S) mutation in a real-world cohort of patients with relapsed/refractory chronic lymphocytic leukaemia during ibrutinib therapy. Br J Haematol. 2021;194(2):355-64.

61. Galimberti S, Balducci S, Guerrini F, Del Re M, Cacciola R. Digital Droplet PCR in Hematologic Malignancies: A New Useful Molecular Tool. Diagnostics (Basel). 2022;12(6).

62. Baker T, Nerle S, Pritchard J, Zhao B, Rivera VM, Garner A, Gonzalvez F. Acquisition of a single EZH2 D1 domain mutation confers acquired resistance to EZH2-targeted inhibitors. Oncotarget. 2015;6(32):32646-55.

63. Lauer EM, Mutter J, Scherer F. Circulating tumor DNA in B-cell lymphoma: technical advances, clinical applications, and perspectives for translational research. Leukemia. 2022.

64. Morin RD, Mendez-Lago M, Mungall AJ, Goya R, Mungall KL, Corbett RD, Johnson NA, Severson TM, Chiu R, Field M, Jackman S, Krzywinski M, Scott DW, Trinh DL, Tamura-Wells J, Li S, Firme MR, Rogic S, Griffith M, Chan S, Yakovenko O, Meyer IM, Zhao EY, Smailus D, Moksa M, Chittaranjan S, Rimsza L, Brooks-Wilson A, Spinelli JJ, Ben-Neriah S, Meissner B, Woolcock B, Boyle M, McDonald H, Tam A, Zhao Y, Delaney A, Zeng T, Tse K, Butterfield Y, Birol I, Holt R, Schein J, Horsman DE, Moore R, Jones SJ, Connors JM, Hirst M, Gascoyne RD, Marra MA. Frequent mutation of histone-modifying genes in non-Hodgkin lymphoma. Nature. 2011;476(7360):298-303.

65. Bodor C, O'Riain C, Wrench D, Matthews J, Iyengar S, Tayyib H, Calaminici M, Clear A, Iqbal S, Quentmeier H, Drexler HG, Montoto S, Lister AT, Gribben JG, Matolcsy A, Fitzgibbon J. EZH2 Y641 mutations in follicular lymphoma. Leukemia. 2011;25(4):726-9.

66. Garcia-Alvarez M, Alonso-Alvarez S, Prieto-Conde I, Jimenez C, Sarasquete ME, Chillon MC, Medina A, Balanzategui A, Maldonado R, Anton A, Rodriguez M, Blanco O, Diaz LG, Tamayo P, Blanco P, Esteban C, Gonzalez-Calle V, Puig N, Gutierrez N, Martin A, Garcia-Sanz R, Gonzalez M, Caballero MD, Alcoceba M. Genetic complexity impacts the clinical outcome of follicular lymphoma patients. Blood Cancer J. 2021;11(1):11.

67. Okosun J, Bodor C, Batlevi C, Nagy N, Michot J, Schneider T, Alizadeh H, Simon Z, Vose J, Younes A, Ribrag V, Fitzgibbon J, Yang J, Agarwal S, Newberry KJ, Michaud NR. EZH2 gain-of-function mutations are not associated with more favorable prognosis in relapsed/refractory follicular lymphoma (FL): a preliminary analysis on 590 patients. Hematological Oncology. 2019;37(S2):192-3.

68. Magnes T, Wagner S, Thorner AR, Neureiter D, Klieser E, Rinnerthaler G, Weiss L, Huemer F, Schlick K, Zaborsky N, Steiner M, Greil R, Egle A, Melchardt T. Spatial Heterogeneity in Large Resected Diffuse Large B-Cell Lymphoma Bulks Analysed by

Massively Parallel Sequencing of Multiple Synchronous Biopsies. Cancers (Basel). 2021;13(4).

69. Rossi D, Diop F, Spaccarotella E, Monti S, Zanni M, Rasi S, Deambrogi C, Spina V, Bruscaggin A, Favini C, Serra R, Ramponi A, Boldorini R, Foa R, Gaidano G. Diffuse large B-cell lymphoma genotyping on the liquid biopsy. Blood. 2017;129(14):1947-57.

70. Camus V, Viennot M, Lequesne J, Viailly PJ, Bohers E, Bessi L, Marcq B, Etancelin P, Dubois S, Picquenot JM, Veresezan EL, Cornic M, Burel L, Loret J, Becker S, Decazes P, Lenain P, Lepretre S, Lemasle E, Lanic H, Menard AL, Contentin N, Tilly H, Stamatoullas A, Jardin F. Targeted genotyping of circulating tumor DNA for classical Hodgkin lymphoma monitoring: a prospective study. Haematologica. 2021;106(1):154-62.

71. Rivas-Delgado A, Nadeu F, Enjuanes A, Casanueva-Eliceiry S, Mozas P, Magnano L, Castrejon de Anta N, Rovira J, Dlouhy I, Martin S, Osuna M, Rodriguez S, Simo M, Pinyol M, Baumann T, Bea S, Balague O, Delgado J, Villamor N, Setoain X, Campo E, Gine E, Lopez-Guillermo A. Mutational Landscape and Tumor Burden Assessed by Cell-free DNA in Diffuse Large B-Cell Lymphoma in a Population-Based Study. Clin Cancer Res. 2021;27(2):513-21.

72. Spina V, Bruscaggin A, Cuccaro A, Martini M, Di Trani M, Forestieri G, Manzoni M, Condoluci A, Arribas A, Terzi-Di-Bergamo L, Locatelli SL, Cupelli E, Ceriani L, Moccia AA, Stathis A, Nassi L, Deambrogi C, Diop F, Guidetti F, Cocomazzi A, Annunziata S, Rufini V, Giordano A, Neri A, Boldorini R, Gerber B, Bertoni F, Ghielmini M, Stussi G, Santoro A, Cavalli F, Zucca E, Larocca LM, Gaidano G, Hohaus S, Carlo-Stella C, Rossi D. Circulating tumor DNA reveals genetics, clonal evolution, and residual disease in classical Hodgkin lymphoma. Blood. 2018;131(22):2413-25.

73. Sarkozy C, Huet S, Carlton VE, Fabiani B, Delmer A, Jardin F, Delfau-Larue MH, Hacini M, Ribrag V, Guidez S, Faham M, Salles G. The prognostic value of clonal heterogeneity and quantitative assessment of plasma circulating clonal IG-VDJ sequences at diagnosis in patients with follicular lymphoma. Oncotarget. 2017;8(5):8765-74.

74. Fernandez-Miranda I, Pedrosa L, Llanos M, Franco FF, Gomez S, Martin-Acosta P, Garcia-Arroyo FR, Guma J, Horcajo B, Ballesteros AK, Galvez L, Martinez N, Marin M, Sequero S, Navarro M, Yanguas-Casas N, Calvo V, Rueda-Dominguez A, Provencio M, Sanchez-Beato M. Monitoring of circulating tumor DNA predicts response to

treatment and early progression in follicular lymphoma: results of a prospective pilot study. Clin Cancer Res. 2022.

75. Camus V, Sarafan-Vasseur N, Bohers E, Dubois S, Mareschal S, Bertrand P, Viailly PJ, Ruminy P, Maingonnat C, Lemasle E, Stamatoullas A, Picquenot JM, Cornic M, Beaussire L, Bastard C, Frebourg T, Tilly H, Jardin F. Digital PCR for quantification of recurrent and potentially actionable somatic mutations in circulating free DNA from patients with diffuse large B-cell lymphoma. Leuk Lymphoma. 2016;57(9):2171-9.

76. McDonald A, Thomas E, Daigle S, Morschhauser F, Salles G, Ribrag V, McKay P, Tilly H, Schmitt A, Batlevi CL, Fruchart C, Johnson P, Dickinson M, Opat S, Jurczak W, Cartron G, Lamy T, Zinzani PL, Assouline S, Radford J, Gribben JG, Haioun C, Chaidos A, Le Gouill S, Clawson A, Larus J, Blakemore SJ. Updated Report on Identification of Molecular Predictors of Tazemetostat Response in an Ongoing NHL Phase 2 Study. Blood. 2018;132:4097.

77. Martinez-Laperche C, Sanz-Villanueva L, Diaz Crespo FJ, Muniz P, Martin Rojas R, Carbonell D, Chicano M, Suarez-Gonzalez J, Menarguez J, Kwon M, Diez Martin JL, Buno I, Bastos Oreiro M. EZH2 mutations at diagnosis in follicular lymphoma: a promising biomarker to guide frontline treatment. BMC Cancer. 2022;22(1):982.

78. Gonzalez-Rincon J, Mendez M, Gomez S, Garcia JF, Martin P, Bellas C, Pedrosa L, Rodriguez-Pinilla SM, Camacho FI, Quero C, Perez-Callejo D, Rueda A, Llanos M, Gomez-Codina J, Piris MA, Montes-Moreno S, Barcena C, Rodriguez-Abreu D, Menarguez J, de la Cruz-Merino L, Monsalvo S, Parejo C, Royuela A, Kwee I, Cascione L, Arribas A, Bertoni F, Mollejo M, Provencio M, Sanchez-Beato M. Unraveling transformation of follicular lymphoma to diffuse large B-cell lymphoma. PLoS One. 2019;14(2):e0212813.

79. Laurent C, Charmpi K, Gravelle P, Tosolini M, Franchet C, Ysebaert L, Brousset P, Bidaut A, Ycart B, Fournie JJ. Several immune escape patterns in non-Hodgkin's lymphomas. Oncoimmunology. 2015;4(8):e1026530.

80. Huet S, Xerri L, Tesson B, Mareschal S, Taix S, Mescam-Mancini L, Sohier E, Carrere M, Lazarovici J, Casasnovas O, Tonon L, Boyault S, Hayette S, Haioun C, Fabiani B, Viari A, Jardin F, Salles G. EZH2 alterations in follicular lymphoma: biological and clinical correlations. Blood Cancer J. 2017;7(4):e555.

81. Schroers-Martin JG, Kurtz DM, Soo J, Jin M, Scherer F, Craig A, Chabon JJ, Liu CL, Stehr H, Duehrsen U, Hüttmann A, Cottereau AS, Meignan M, Casasnovas O, Westin JR, Gaidano G, Rossi D, Advani RH, Roschewski M, Wilson WH, Diehn M, Alizadeh AA. Determinants of Circulating Tumor DNA Levels across Lymphoma Histologic Subtypes. Blood. 2017;130(Supplement 1):4018-.

82. Scherer F, Kurtz DM, Newman AM, Stehr H, Craig AF, Esfahani MS, Lovejoy AF, Chabon JJ, Klass DM, Liu CL, Zhou L, Glover C, Visser BC, Poultsides GA, Advani RH, Maeda LS, Gupta NK, Levy R, Ohgami RS, Kunder CA, Diehn M, Alizadeh AA. Distinct biological subtypes and patterns of genome evolution in lymphoma revealed by circulating tumor DNA. Sci Transl Med. 2016;8(364):364ra155.

83. Roschewski M, Dunleavy K, Pittaluga S, Moorhead M, Pepin F, Kong K, Shovlin M, Jaffe ES, Staudt LM, Lai C, Steinberg SM, Chen CC, Zheng J, Willis TD, Faham M, Wilson WH. Circulating tumour DNA and CT monitoring in patients with untreated diffuse large B-cell lymphoma: a correlative biomarker study. Lancet Oncol. 2015;16(5):541-9.

84. Delfau-Larue MH, van der Gucht A, Dupuis J, Jais JP, Nel I, Beldi-Ferchiou A, Hamdane S, Benmaad I, Laboure G, Verret B, Haioun C, Copie-Bergman C, Berriolo-Riedinger A, Robert P, Casasnovas RO, Itti E. Total metabolic tumor volume, circulating tumor cells, cell-free DNA: distinct prognostic value in follicular lymphoma. Blood Adv. 2018;2(7):807-16.

85. Distler A, Lakhotia R, Phelan JD, Pittaluga S, Melani C, Muppidi JR, Simard J, Pradhan A, Hillsman A, Yang Y, Davies-Hill T, Shaffer AL, III, Evans S, Ahlman MA, Jacob AP, Bagaev A, Meerson M, Postovalova E, Kudryashova O, Kotlov N, Fowler NH, Jaffe ES, Staudt LM, Wilson WH, Roschewski M. A Prospective Study of Clonal Evolution in Follicular Lymphoma: Circulating Tumor DNA Correlates with Overall Tumor Burden and Fluctuates over Time without Therapy. Blood. 2021;138(Supplement 1):1328-.

86. Kurtz DM, Scherer F, Jin MC, Soo J, Craig AFM, Esfahani MS, Chabon JJ, Stehr H, Liu CL, Tibshirani R, Maeda LS, Gupta NK, Khodadoust MS, Advani RH, Levy R, Newman AM, Duhrsen U, Huttmann A, Meignan M, Casasnovas RO, Westin JR, Roschewski M, Wilson WH, Gaidano G, Rossi D, Diehn M, Alizadeh AA. Circulating

Tumor DNA Measurements As Early Outcome Predictors in Diffuse Large B-Cell Lymphoma. J Clin Oncol. 2018;36(28):2845-53.

87. Kurtz DM, Soo J, Co Ting Keh L, Alig S, Chabon JJ, Sworder BJ, Schultz A, Jin MC, Scherer F, Garofalo A, Macaulay CW, Hamilton EG, Chen B, Olsen M, Schroers-Martin JG, Craig AFM, Moding EJ, Esfahani MS, Liu CL, Duhrsen U, Huttmann A, Casasnovas RO, Westin JR, Roschewski M, Wilson WH, Gaidano G, Rossi D, Diehn M, Alizadeh AA. Enhanced detection of minimal residual disease by targeted sequencing of phased variants in circulating tumor DNA. Nat Biotechnol. 2021;39(12):1537-47.

88. Lakhotia R, Melani C, Dunleavy K, Pittaluga S, Saba N, Lindenberg L, Mena E, Bergvall E, Lucas AN, Jacob A, Yusko E, Steinberg SM, Jaffe ES, Wiestner A, Wilson WH, Roschewski M. Circulating tumor DNA predicts therapeutic outcome in mantle cell lymphoma. Blood Adv. 2022;6(8):2667-80.

89. Kurtz DM, Green MR, Bratman SV, Scherer F, Liu CL, Kunder CA, Takahashi K, Glover C, Keane C, Kihira S, Visser B, Callahan J, Kong KA, Faham M, Corbelli KS, Miklos D, Advani RH, Levy R, Hicks RJ, Hertzberg M, Ohgami RS, Gandhi MK, Diehn M, Alizadeh AA. Noninvasive monitoring of diffuse large B-cell lymphoma by immunoglobulin high-throughput sequencing. Blood. 2015;125(24):3679-87.

90. Pott C, Wellnitz D, Ladetto M. Minimal residual disease in follicular lymphoma. Annals of Lymphoma. 2021;5.

91. Zohren F, Bruns I, Pechtel S, Schroeder T, Fenk R, Czibere A, Maschmeyer G, Kofahl-Krause D, Niederle N, Heil G, Losem C, Welslau M, Brugger W, Germing U, Kronenwett R, Barth J, Rummel MJ, Haas R, Kobbe G. Prognostic value of circulating Bcl-2/IgH levels in patients with follicular lymphoma receiving first-line immunochemotherapy. Blood. 2015;126(12):1407-14.

IX. Bibliography

Publications in connection with the thesis

1. Nagy A, Batai B, Balogh A, Illes S, Mikala G, Nagy N, Kiss L, Kotmayer L, Matolcsy A, Alpar D, Masszi T, Masszi A, Bodor C. Quantitative Analysis and Monitoring of EZH2 Mutations Using Liquid Biopsy in Follicular Lymphoma. Genes (Basel). 2020;11(7). **IF: 4,141**
2. Nagy A, Batai B, Kiss L, Grof S, Kiraly PA, Jona A, Demeter J, Santa H, Batai A, Pettendi P, Szendrei T, Plander M, Korosmezey G, Alizadeh H, Kajtar B, Mehes G, Krenacs L, Timar B, Csomor J, Toth E, Schneider T, Mikala G, Matolcsy A, Alpar D, Masszi A, Bodor C. Parallel testing of liquid biopsy (ctDNA) and tissue biopsy samples reveals a higher frequency of EZH2 mutations in follicular lymphoma. J Intern Med. 2023. **IF: 13,068**
3. Nagy Á, Bátai B, Kiss L, Marx A, Pinczés LI, Papp G, Kacskovics I, Alpár D, Bodor C. Potential applications of liquid biopsy analyses in oncohematology. [Hungarian]. Hematológia–Transzfuziológia. 2020;53(3):144-56.
4. Nagy Á, Levey L, Zajta E, Gergő P. Potential applications of liquid biopsy analyses in solid tumors. [Hungarian]. Orvosképzés. 2021;46(3):12.

Publications independent of the thesis

1. Furedi N, Nagy A, Miko A, Berta G, Kozicz T, Petervari E, Balasko M, Gaszner B. Melanocortin 4 receptor ligands modulate energy homeostasis through urocortin 1 neurons of the centrally projecting Edinger-Westphal nucleus. Neuropharmacology. 2017;118:26-37. **IF: 5,273**
2. Fésüs V, Nagy Á, Alpár D, Bodor C. Az adoptív sejttranszfer sikere a hematológiában: a kiméra antigénreceptorral felruházott T-sejtek. Hematológia–Transzfuziológia. 2019;52(3):178.
3. Gango A, Alpar D, Galik B, Marosvari D, Kiss R, Fesus V, Aczel D, Eyupoglu E, Nagy N, Nagy A, Krizsan S, Reiniger L, Farkas P, Kozma A, Adam E, Tasnady S, Reti M, Matolcsy A, Gyenesei A, Matrai Z, Bodor C. Dissection of subclonal evolution by temporal mutation profiling in chronic lymphocytic leukemia patients treated with ibrutinib. Int J Cancer. 2020;146(1):85-93. **IF: 7,316**

4. Bodor C, Alpar D, Marosvari D, Galik B, Rajnai H, Batai B, Nagy A, Kajtar B, Burjan A, Deak B, Schneider T, Alizadeh H, Matolcsy A, Brandner S, Storhoff J, Chen N, Liu M, Ghali N, Csala I, Bago AG, Gyenesei A, Reiniger L. Molecular Subtypes and Genomic Profile of Primary Central Nervous System Lymphoma. J Neuropathol Exp Neurol. 2020;79(2):176-83. **IF: 3,148**
5. Nagy Á, Andrikovics H, Kajtár B, Ujfalusi A, László Z, Kotmayer L, Csabán D, Bors A, Makkos-Weisz A, Kapitány E, Sulák A, Bodor C. Az IGHV-mutációs státusz vizsgálata a Magyar Hematológiai és Transzfuziológiai Társaság Molekuláris Diagnosztika Munkacsoportjának laboratóriumaiban. Hematológia–Transzfuziológia. 2021;54(2):75-80.
6. Kiss L, Bátai B, Bodor C, Nagy Á. Új molekuláris klasszifikációs rendszerek diffúz nagy B-sejtes limfómában. Hematológia–Transzfuziológia. 2021;54(2):104-12.
7. Schvarcz CA, Danics L, Krenacs T, Viana P, Beres R, Vancsik T, Nagy A, Gyenesei A, Kun J, Fonovic M, Vidmar R, Benyo Z, Kaucsar T, Hamar P. Modulated Electro-Hyperthermia Induces a Prominent Local Stress Response and Growth Inhibition in Mouse Breast Cancer Isografts. Cancers (Basel). 2021;13(7). **IF: 6,575**
8. Sebestyen E, Nagy A, Marosvari D, Rajnai H, Kajtar B, Deak B, Matolcsy A, Brandner S, Storhoff J, Chen N, Bago AG, Bodor C, Reiniger L. Distinct miRNA Expression Signatures of Primary and Secondary Central Nervous System Lymphomas. J Mol Diagn. 2022;24(3):224-40. **IF: 5,341**
9. Agoston EI, Acs B, Herold Z, Fekete K, Kulka J, Nagy A, Muhl D, Mohacsi R, Dank M, Garay T, Harsanyi L, Gyorffy B, Szasz AM. Deconstructing Immune Cell Infiltration in Human Colorectal Cancer: A Systematic Spatiotemporal Evaluation. Genes (Basel). 2022;13(4). **IF: 4,141**
10. Almasi S, Kuthi L, Sejben A, Voros A, Nagy A, Zombori T, Cserni G. TRPS1 expression in cytokeratin 5 expressing triple negative breast cancers, its value as a marker of breast origin. Virchows Arch. 2023;482(5):861-8. **IF: 4,548**
11. Marx A, Osvath M, Szikora B, Pipek O, Csabai I, Nagy A, Bodor C, Matula Z, Nagy G, Bors A, Uher F, Mikala G, Valyi-Nagy I, Kacskovics I. Liquid biopsy-based monitoring of residual disease in multiple myeloma by analysis of the rearranged immunoglobulin genes-A feasibility study. PLoS One. 2023;18(5):e0285696. **IF: 3,752**

X. Acknowledgements

First, I would like to express my gratitude towards my family, to my parents and to my brother who always supported me throughout my studies.

I would like to thank all the support and help to my PhD tutor, Csaba Bödör, to whom I could always turn for help and for advice.

I would like to thank Noémi Nagy for teaching me the fundamental laboratory techniques at the beginning of my PhD work.

I am grateful for the lot of help, support and for the friendly environment from the members of our research group. I owe special thanks to Bence Bátai, with whom we created an effective lymphoma team and with whom we always helped and supported each other's projects.

I would like to also thank the tremendous help what I have received from members of the routine diagnostic part of our oncohematological laboratory. I am sincerely grateful to Stefánia Gróf who was always very helpful with the wet lab experiments whenever it was needed. I very much appreciate the help of Adrienne Pallag who supported the study with the sectioning of the FFPE tissue blocks.

I am grateful for the work of the TDK students, who were very helpful with the initial sample processing steps. Here, I would like to mention Laura Kiss, who worked on this research with me for more than four years.

I am also grateful for all the members of the Department of Pathology and Experimental Cancer Research, hence everyone contributed to my PhD work during the last five years.

Last but not least, I would like to thank for all the Hungarian Hematologists and Pathologist who contributed with blood and tissue samples to this study, with their help, we could really accomplish a nationwide collaboration for the support of this research.